Department of Mechanical Engineering

# Low-velocity impact damage in fibre metal laminates

## a study of the impact resistance and metal-composite debonding

Tuomas Pärnänen

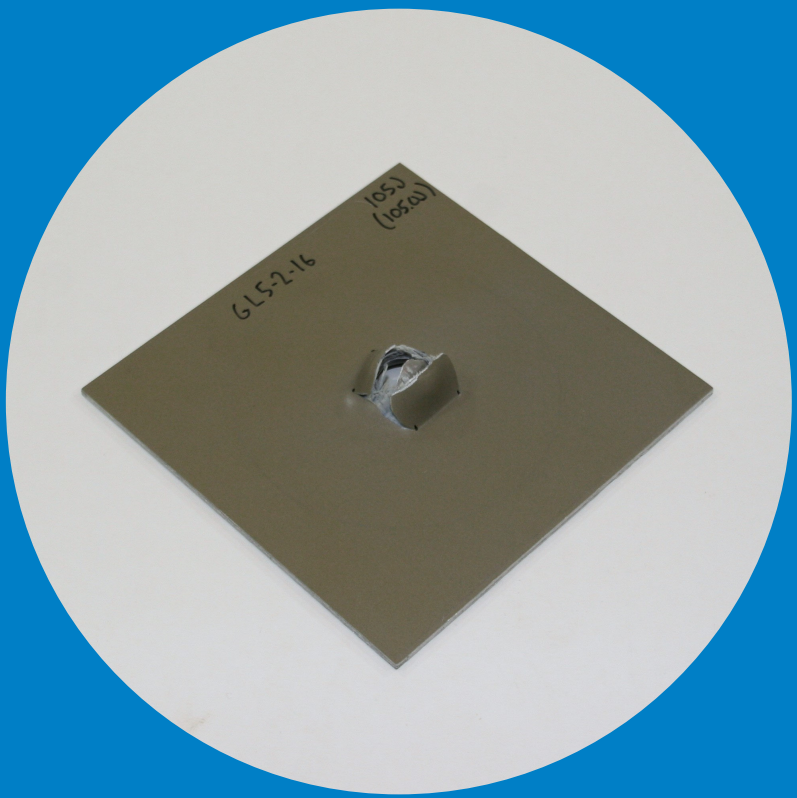


Aalto University

DOCTORAL DISSERTATIONS

Aalto University publication series
**DOCTORAL DISSERTATIONS** 262/2016

# Low-velocity impact damage in fibre metal laminates

a study of the impact resistance and metal-composite debonding

**Tuomas Pärnänen**

A doctoral dissertation completed for the degree of Doctor of Science (Technology) to be defended, with the permission of the Aalto University School of Engineering, at a public examination held at the lecture hall 216 of the school on 27th January 2017 at 12.

**Aalto University**
**School of Engineering**
**Department of Mechanical Engineering**

**Supervising professor**
Prof. Olli Saarela, Aalto University, Finland

**Thesis advisor**
Prof. Mikko Kanerva, Tampere University of Technology, Finland

**Preliminary examiners**
Prof. Javid Bayandor, Virginia Tech, USA
Prof. Jeremy Laliberté, Carleton University, Canada

**Opponent**
Prof. Wesley Cantwell, Khalifa University, United Arab Emirates

Aalto University publication series
**DOCTORAL DISSERTATIONS** 262/2016



ISBN 978-952-60-7189-3 (printed)
ISBN 978-952-60-7188-6 (pdf)
ISSN-L 1799-4934
ISSN 1799-4934 (printed)
ISSN 1799-4942 (pdf)
http://urn.fi/URN:ISBN:978-952-60-7188-6

Unigrafia Oy
Helsinki 2016

Finland

441 697
Printed matter

Aalto University

# Abstract

Aalto University, P.O. Box 11000, FI-00076 Aalto www.aalto.fi

**Author**
Tuomas Pärnänen

**Name of the doctoral dissertation**
Low-velocity impact damage in fibre metal laminates – a study of the impact resistance and metal-composite debonding

**Publisher** School of Engineering

**Unit** Department of Mechanical Engineering

**Series** Aalto University publication series DOCTORAL DISSERTATIONS 262/2016

**Field of research** Aeronautical Engineering

**Manuscript submitted** 20 June 2016 **Date of the defence** 27 January 2017

**Permission to publish granted (date)** 14 November 2016 **Language** English

☐ **Monograph** ☒ **Article dissertation** ☐ **Essay dissertation**

**Abstract**

Fibre metal laminates (FMLs) refer to a hybrid material concept that combines layers of thin metal sheets and fibre-reinforced plastics. This thesis concentrates on the damage characteristics of FMLs subjected to collision-type low-velocity impacts. The damage characteristics are studied by drop-weight impact and quasi-static indentation experiments and using finite element simulations.

The work is divided into two parts. In Part I, specific interest is laid on the impact resistance of AZ31B-H24 magnesium alloy-based FMLs. The results indicate a disadvantage for the magnesium alloy, as the impact energy limits for metal cracking are significantly lower when compared to the state-of-the-art FML structure Glare 5 with 2024-T3 aluminium alloy layers. The main reason for the difference in cracking energies is concluded to result from the metal tensile response over the plastic region. The lower rate of strain hardening for the magnesium alloy enhances the local strain accumulation over the impact point, which leads to premature cracking. In addition, the impact damage process is experimentally studied in Part I by using a wide range of impact energies. The purpose of the damage process study is to gain an overall view of the impact damage evolution in FMLs. Finally, impacts on FMLs are studied via finite element simulations.

Part II focuses on the debonding occurring in FMLs during impact loading, i.e. on the damage process along the metal-composite interface. The study reveals that the debond at the lowermost metal-composite interface forms in two stages. During the impactor loading phase, a debond tends to form as a fracture mode II cracking caused by out-of-plane shear forces. As the impactor rebound phase follows, the linear-elastic composite layers force the FML to straighten. On the contrary, the lowermost metal sheet has deformed plastically and tends to maintain its deformed shape. The discrepancy in the material response leads to peeling forces and consequently to fracture mode I dominated debonding.

In the current literature, the debonding along the metal-composite interface is not commonly taken into account in the impact damage modelling of FMLs, and at times the debonding by shear forces is only considered. The energy absorption by the debonding may not be significant in the impact process, but the results of this thesis indicate that the debonding substantially affects deformations and the post-impact strain state. A realistic prediction of the post-impact damage state is especially important for successful investigations of damage tolerance. Therefore, a modelling methodology that takes into account the debonding with the described two-stage formation process defined in this thesis is suggested for future models.

**Keywords** fibre metal laminates, hybrids, impact, impact resistance, debonding

**ISBN (printed)** 978-952-60-7189-3 **ISBN (pdf)** 978-952-60-7188-6

**ISSN-L** 1799-4934 **ISSN (printed)** 1799-4934 **ISSN (pdf)** 1799-4942

**Location of publisher** Helsinki **Location of printing** Helsinki **Year** 2016

**Pages** 120 **urn** http://urn.fi/URN:ISBN:978-952-60-7188-6

**Tekijä**
Tuomas Pärnänen

**Väitöskirjan nimi**
Lujitemuovi-metalli-yhdistelmälaminaattien iskuvaurioituminen – tutkimus iskunkestävyydestä ja kerrostenvälisestä murtumisesta

**Julkaisija** Insinööritieteiden korkeakoulu

**Yksikkö** Konetekniikan laitos

**Sarja** Aalto University publication series DOCTORAL DISSERTATIONS 262/2016

**Tutkimusala** Lentotekniikka

**Käsikirjoituksen pvm** 20.06.2016 **Väitöspäivä** 27.01.2017

**Julkaisuluvan myöntämispäivä** 14.11.2016 **Kieli** Englanti

☐ **Monografia** ☒ **Artikkeliväitöskirja** ☐ **Esseeväitöskirja**

**Tiivistelmä**

Lujitemuovi-metalli-yhdistelmälaminaatit (jatkossa laminaatit) ovat rakenteita, jotka muodostuvat ohuista metalli- ja lujitemuovikerroksista. Tässä väitöskirjassa tutkitaan laminaattien vaurioitumista hitaiden törmäystyyppisten iskujen vaikutuksesta. Iskuvaurioitumista tutkitaan pudotus- ja painamiskokein sekä elementtimenetelmään perustuvilla simulaatioilla.

Työn ensimmäisessä osassa tutkitaan erityisesti AZ31B-H24 magnesiumkerroksia sisältävien laminaattien iskunkestävyyttä. Tulosten mukaan laminaatin iskunkestävyys on 2024-T3 alumiinikerroksia sisältävää Glare 5 -laminaattia heikompi. Iskunkestävyyden lisäksi ensimmäisessä osassa tutkitaan iskuvaurioiden kehittymistä tarkastelemalla eri iskuenergioilla kuormitettujen koekappaleiden vaurioita. Lopuksi laminaattien iskukuormittumista tutkitaan elementtimenetelmään perustuvilla simulaatioilla.

Työn toisessa osassa keskitytään kerrostenväliseen murtumiseen, joka tapahtuu metallien ja lujitemuovien rajapinnassa. Työn tulokset osoittavat, että murtuminen laminaatin alimmaisessa rajapinnassa tapahtuu iskun aikana kahdessa eri vaiheessa. Iskun alkuvaiheessa murtuma muodostuu laminaatin normaalin suuntaisten leikkausvoimien seurauksena. Iskun paluuvaiheen aikana lujitemuovikerrokset pyrkivät suoristumaan plastisesti muovautuneita metallikerroksia enemmän. Ero materiaalivasteessa johtaa repivään kuormitukseen ja murtumiseen.

Rajapinnan murtumista ei tyypillisesti ole otettu huomioon iskumalleissa ja toisinaan ainoastaan leikkausvoimista aiheutuva murtuminen on huomioitu. Väitöskirjan tulokset osoittavat, että kaksivaiheinen murtuminen vaikuttaa merkittävästi laminaatin muodonmuutoksiin ja iskunjälkeiseen venymätilaan. Realistinen vauriotilan määrittäminen on erityisen tärkeää iskunjälkeistä lujuutta tarkasteltaessa. Tämän vuoksi jatkossa on suositeltavaa ottaa huomioon kaksivaiheinen murtuminen laminaattien iskukuormitusta mallinnettaessa.

**Avainsanat** yhdistelmälaminaatit, iskunkestävyys, kerrostenvälinen murtuminen

**ISBN (painettu)** 978-952-60-7189-3 **ISBN (pdf)** 978-952-60-7188-6

**ISSN-L** 1799-4934 **ISSN (painettu)** 1799-4934 **ISSN (pdf)** 1799-4942

**Julkaisupaikka** Helsinki **Painopaikka** Helsinki **Vuosi** 2016

**Sivumäärä** 120 **urn** http://urn.fi/URN:ISBN:978-952-60-7188-6

# Preface

During my studies, I have received funding from the Finnish Funding Agency for Technology and Innovation through the K3MAT project (2010-2011), the National Graduate School in Engineering Mechanics (2013-2016), Aalto University School of Engineering and Walter Ahlström foundation. Their financial support is gratefully acknowledged. I would also like to acknowledge VTT Expert Services Oy, Patria Aerostructures Oy, Outokumpu Oyj and Kromatek Ab for their support to the experimental part of the work.

I am lucky to have worked with a number of great people during the dissertation process. The main part of the research was carried out in the Laboratory of Lightweight Structures in Aalto University. Firstly, I thank my supervisor Olli Saarela for the opportunity to join his group, as well as for his support and trust in my work. I am forever grateful to my advisor Mikko Kanerva for his dedication to my project and his encouragement to challenge myself. I also thank all my colleagues for creating a supportive working environment and offering help whenever I have needed it. Especially, I thank Jarno Jokinen for the fruitful discussions about finite element modelling.

I was fortunate to work as a visiting researcher in TU Delft Faculty of Aerospace Engineering in 2010. I express my gratitude to René Alderliesten for the guidance and valuable discussions during my visit. I also thank Mojtaba Sadighi, Freddy Morinière and Calvin Rans for sharing their ideas and thoughts about my research. I have great memories from my time in the Netherlands. For this, I thank my colleagues and friends in TU Delft.

I express my gratitude to the group of Marine Technology of Aalto University for providing a helping hand when I needed it. Especially, I thank Jani Romanoff for his support and encouragement during the final part of my work. Thanks go also to my colleagues in Tampere University of Technology. It has been great fun to do science together. Last but not least, I thank Kim-Niklas Antin from Aalto University for creating an interesting environment to learn advanced structures in practice.

I thank my pre-examiners Jeremy Laliberté end Javid Bayandor for their effort and thoughtful feedback on this thesis. I am grateful to Wesley Cantwell for kindly agreeing to act as the opponent of this thesis.

Finally, I express my deepest gratitude to my parents, sisters, family and friends for their unconditional help and support. Especially, I am grateful to Katja for her patience and care. Lastly, I thank my daughter Eveliina for bringing joy and laughter to our lives. I'm really proud of you Eve!

Jyväskylä, November 2016
Tuomas Pärnänen

# Contents

# List of Publications

This doctoral dissertation consists of a summary and the following publications (referred to as P1, P2, P3 and P4).

**1.** Pärnänen, Tuomas; Alderliesten, René; Rans, Calvin; Brander, Timo; Saarela, Olli. (2012). Applicability of AZ31B-H24 magnesium in Fibre Metal Laminates – An experimental impact research. Elsevier. Composites Part A: Applied Science and Manufacturing, Volume 43, Issue 9, pages 1578-1586. ISSN of journal 1359-835X. DOI of article 10.1016/j.compositesa.2012.04.008.

**2.** Sadighi, Mojtaba; Pärnänen, Tuomas; Alderliesten, René; Sayeaftabi, Mojtaba; Benedictus, Rinze. (2012). Experimental and Numerical Investigation of Metal Type and Thickness Effects on the Impact Resistance of Fiber Metal Laminates. Springer. Applied Composite Materials, Volume 19, Issue 3-4, pages 545-559. ISSN of journal 0929-189X. DOI of article 10.1007/s10443-011-9235-6.

**3.** Pärnänen, Tuomas; Kanerva, Mikko; Sarlin, Essi; Saarela, Olli. (2015). Debonding and impact damage in stainless steel fibre metal laminates prior to metal fracture. Elsevier. Composite Structures, Volume 119, pages 777-786. ISSN of journal 0263-8223. DOI of article 10.1016/j.compstruct.2014.09.056.

**4.** Pärnänen, Tuomas; Vänttinen, Aki; Kanerva, Mikko; Jokinen, Jarno; Saarela, Olli. (2016). The effect of debonding on the low-velocity impact response of steel-CFRP fibre metal laminates. Applied Composite Materials, Volume 23, Issue 6, pages 1151-1166. DOI of article 10.1007/s10443-016-9505-4.

# Author's Contribution

**Publication 1:** The author conducted the experiments, analysed the results and prepared the manuscript. Alderliesten, Rans, Brander and Saarela contributed the manuscript with valuable ideas, comments and suggestions.

**Publication 2:** The author conducted the experimental part of the research and related reporting in the article. Sayeftabi and Sadighi performed the FE analysis and Sadighi was the corresponding author. Alderliesten and Benedictus contributed the manuscript with valuable ideas, comments and suggestions.

**Publication 3:** The author, together with Kanerva, conducted the experimental part of the work and prepared the manuscript. Kanerva performed the AFM measurements and Sarlin the FESEM imaging. Saarela contributed to the manuscript with valuable comments and suggestions.

**Publication 4:** The author, together with Kanerva, conducted the experiments. The author also conducted the FE simulations and prepared the manuscript. Vänttinen interpreted the DIC results and Jokinen helped to develop the FE model. Vänttinen, Kanerva, Jokinen and Saarela contributed to the manuscript with valuable comments and suggestions.

# Original features

The following features are believed to be original in this thesis:

1) The influence of metal layers on the impact resistance of fibre metal laminates (FMLs) was analysed. The applicability of AZ31B-H24 for FMLs was studied through impact energy limits needed for metal cracking. The test results for the magnesium alloy-based FML were compared with the test results for the Glare 5 FMLs. The results showed a disadvantage for the magnesium alloy-based FML, as the energy limits for metal cracking were significantly lower. The main reason for the difference in cracking energies was concluded as resulting from the tensile stress–strain response of the metal over the plastic region. The low rate of strain hardening for the magnesium alloy enhances the strain accumulation over the impact point, which leads to premature cracking.
2) The debonding at the lowermost metal-composite interface in FMLs was studied using experiments and finite element simulations. The debonding was found to initiate during the loading phase of the impact event as a result of shearing loads (fracture mode II cracking). Additionally, peeling loads cause fracture mode I -dominated debonding during the unloading phase. The discrepancy in the material response between the constituent layers (elastic-plastic metal and linear-elastic composite) is the cause for the peeling loads.
3) The effects of the debonding on the impact response were studied. The debonding during the loading phase of the impact event was shown to reduce the curve slope of the impactor contact force–central deflection response, i.e. to lower bending rigidity. The debonding during the unloading phase influenced the end part of the unloading curve by amplifying the rebound, i.e. by decreasing the final deflection.
4) The post-impact strain field on the lower surface of a stainless steel-based FML was characterised. The results revealed a highly strain-accumulated area around the impact point ($r < 5$ mm). In addition, the effects of the debonding on the peripheral and radial strain components at the FMLs lower surface were studied. The debonding decreased the peripheral strain and resulted in a positive change in the radial strain.

# 1. Introduction

## 1.1 Fibre metal laminates (FMLs)

Fibre metal laminates (FMLs) are laminated hybrid structures, which combine thin metal sheets and fibre-reinforced plastic (FRP) layers, see Fig. 1.1 (Vlot et al., 1999; Vogelesang and Vlot, 2000; Wu, 2005). The layers are bonded together by using additional adhesive films between the metals and FRP composites or by using the matrix material of the FRP layers. FMLs were developed during the 1980s for aeronautical applications to improve the damage tolerance of structures. The fundamental idea was to increase the fatigue life of metallic sheet structures by adding fibre layers into the structures. As the fatigue cracking initiates and propagates in the metal layers, the loading remains transferred through the fibres. What follows is that the crack propagation is remarkably slower when compared to pure metallic structures (Marissen, 1988; Alderliesten and Homan, 2006). Later, when compared to the rival metallic and FRP composite structures, high resistance against collision-type impact loading was highlighted for certain FMLs (Vlot, 1991). Today, the most remarkable application of FMLs is in the Airbus A380-800 airliner, where the upper parts of the fuselage as well as the leading edges of the empennage are manufactured of Glare® FML panels, which combine S2-glass/epoxy and 2024-T3 aluminium alloy layers.

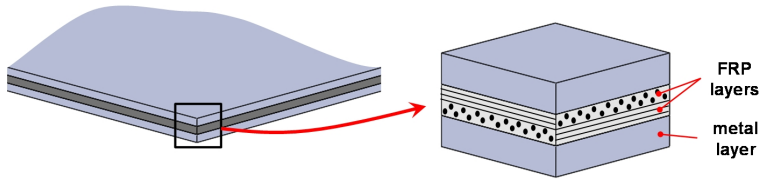


**Figure 1.1.** An example of an FML hybrid panel, which combines metal and FRP layers.

## 1.2 Impact loading on FMLs

An impact in the current context is defined as a collision of a moving object or projectile on a plate structure (Fig. 1.2). The impact by an external object generates complex loading inside the panel structure (Hagenbeek, 2001). Under the contact area, compression loading is formed as the projectile compresses the structure in the thickness direction. Simultaneously, out-of-plane shear loading begins to affect outside of the contact area of the projectile. Moreover, bending

is involved in the deflection process, and therefore in-plane tension and compression stresses are generated in the panel. Finally, membrane tension is formed throughout the panel plane. The intensity of the membrane loading is highly affected by the types of boundary conditions applied to the panel.

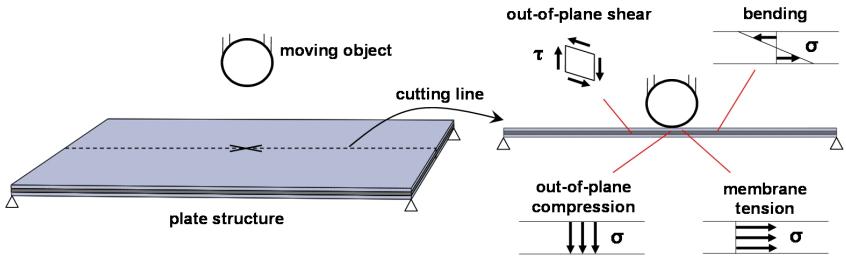


**Figure 1.2.** Impact loading on a plate structure and the types of loading generated by the contact.

Different impacts on a plate structure are primarily divided into three categories by the velocity of an impacting object: (1) low-velocity (<10 m/s), (2) high-velocity (10-100 m/s), and (3) hyper-velocity (km/s) impacts. The panel response to a low-velocity impact often resembles the response to a quasi-static indentation loading as the panel basically deforms in a similar manner, i.e. the panel deflection and loading at the impact point are in phase. The main difference between the quasi-static indentation and low-velocity impact, in addition to wave propagation due to contact, is the panel response due to increased strain rates. An increased strain rate might change the response of the constituent materials. As the collision velocity increases, the dynamic effects increasingly participate in the process. The travelling wave has no time to reach the support boundary during the impact event and, thereby the panel deflection and loading will be out of phase.

When considering the performance of a panel against impact loading, the definition of the performance needs to be clearly stated. For the definition purpose, there are three concepts within impact engineering: impact resistance, impact damage resistance, and impact tolerance (ASTM D5628, 2010; ASTM D7136, 2005; ASTM D7137, 2005). The impact resistance is typically perceived as an (impact energy) limit at which a certain failure happens, for example when first metal cracking appears in FMLs. The impact damage resistance refers to the size of the damage after a specific impact event. Thus, laminates may be impacted by a certain impact energy and ranked by the extension of the damage area. The damage tolerance refers to the structure's residual strength after an impact event, e.g. fatigue life, ultimate strength, or buckling strength of an impacted structure. In addition to the aspects mentioned above, certain applications may have specific requirements for energy absorption or deformation during an impact loading.

Given that FMLs originally are shell materials for airplanes, examples for the impacts on FMLs can be taken from the service of an aircraft (Vlot, 1991; Sadighi

et al., 2012; Morinière, 2014). Aircraft structures are especially susceptible to impacts because a high level of weight optimization is involved in the design and the targeted margins for failure are relatively low. Low-velocity impacts are the most frequent source of impact damage in airliners (Vlot, 1991). Typical low-velocity impacts or indentation-type contacts originate from manufacturing and maintenance (for example due to tool drops). Collisions of ground service cars on fuselages are common, especially around the doors (Vlot, 1991; Morinière, 2014). Cargo floor panels are also impact-prone structures, as the loading of payload tends to cause impacts. In the higher velocity regime, impacts may occur, for example, by bird collisions and hail storms, during the flight.

The full impact damage process in FMLs features composite and metal damaging. The damaging of composites includes matrix cracking, delaminations and fibre failures, whereas the metal layers damage through plastic deformation and metal cracking (Fig. 1.3). As the FML structure is bonded to form a laminate, metal and FRP layers can also separate from each other. This additional damage mode is called “debond”. The process when the debond forms is called “debonding”.

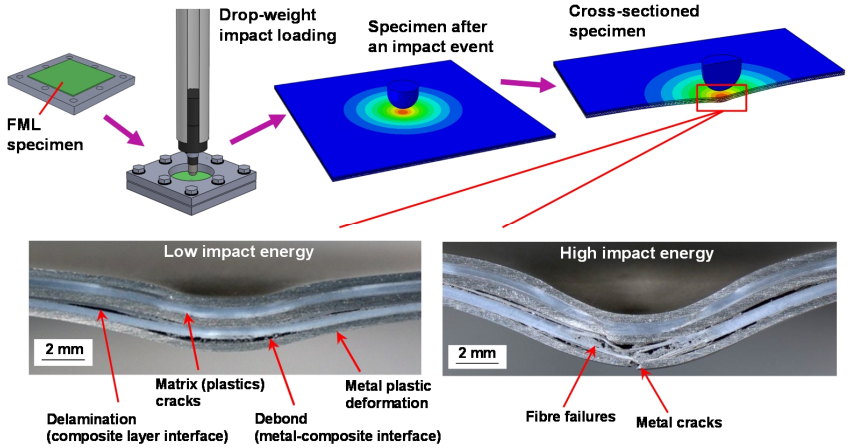


**Figure 1.3.** Primary damage modes found in a type 3/2 (3 layers of metal and 2 sections of FRP composite) FML specimen after drop-weight impact loading.

An intrinsic objective of impact engineering is to gain knowledge for designing impact resistant and impact tolerant structures (see Fig. 1.4). The real key for good design is to understand the interaction of different damage modes involved in the impact damage process. Before initiating any extensive study for damage interaction, the formation mechanisms of each damage mode need to be explained. To be precise, we need to understand why these damages are generated at certain locations. There is a gap especially in the knowledge of debonding mechanisms of FMLs in the current literature.

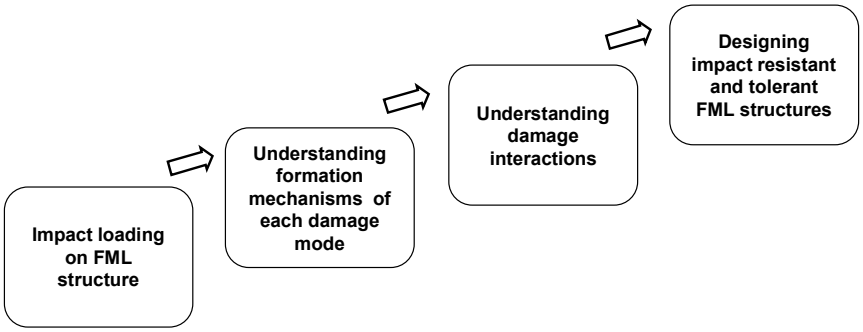


**Figure 1.4.** The research steps needed for gaining the knowledge to design impact resistant and tolerant FML structures.

## 1.3 Scope and objectives of the work

This research investigates the impact resistance, impact damage process, impact response and debonding in FMLs subjected to low-velocity impact loading. The findings of this research are gained through experimental drop-weight impact and indentation tests and with finite element simulations.

In Part I, the impact resistance, impact damage process and impact response of FMLs are studied. In brief, Part I addresses the following questions:

- How is the impact resistance related to the tensile stress-strain response of a metal layer?
- How does the impact damage evolve along with the increased impact energy?
- How to model impact response (i.e., the contact force–central deflection response) computationally?

In Part II, the debonding and its effects on the impact response are studied. The study focuses on low-energy impact loading when the presence of other damage modes is at a minimum. Part II addresses the following questions for FMLs:

- How and in which locations does debond initiate during impact loading?
- How does debond propagate during impact loading?
- How is the debond crack tip loaded during impact loading (by shearing, by peeling, or by shearing and peeling)?
- How does the debonding affect the impact response and free surface straining?

## 1.4 Dissertation structure

The dissertation includes a summary part and four original research articles. Part I (P1, P2) concerns the impact resistance, impact damage process and impact response of FMLs. The impact resistance and damage process are studied by drop-weight impact experiments (P1, P2). The impact resistance is examined from the aspect of metal layer cracking. A specific interest is to study the applicability of AZ31B-H24 magnesium alloy in FMLs (type 3/2 stacking). The impact resistance characteristics of the magnesium based FML are studied together with the state-of-the-art FML structure Glare 5. The impact damage process is examined by studying damage patterns of the specimens after impact loading (P1, P2). The experiments use impact energies from small up to full perforation. Finally, finite element models are created to study the impact response of FMLs (P2).

Part II (P3, P4) focuses on the debonding in FMLs during low-velocity impact loading. The structure of the FML specimen here is a simpler type 2/1 stacking with stainless steel metal layers. Ductile stainless steel sheets are utilized in order to postpone metal cracking and to gain better focus on the debond damage mode. First, an experimental research (P3) is carried out to study debond patterns in low impact energy specimens. Next, finite element models are created to study the debonding mechanisms of FMLs (P4). In addition, the effects of the debonding on the impact response and free surface straining are studied (P4).

# 2. Theoretical background

## 2.1 Overview of low-velocity impact and impact resistance research on FMLs

Composite laminates made of fibre-reinforced plastic (FRP) layers are susceptible to impact loading. Therefore, their impact damage mechanisms have been studied extensively in the literature (e.g. Cantwell and Morton, 1991; Richardson and Wisheart, 1996; Hou et al.; 2000; Abrate, 2001; Bayandor et al., 2003; Davies and Olsson, 2004; Shi et al., 2012). Consequently, many of the approaches used for studying impact response of FMLs originate from these studies.

In the first extensive study about the effects of impact loading on FMLs, Vlot (1991) found that certain FML lay-ups persist higher impact resistance when compared to rival metal or composite panels suited for aerostructures. Since then, a large number of experimental studies have been performed to find more impact-resistant FMLs by comparing the performance of different materials and stacking combinations. Primarily, unidirectional or cross-plied stacking for the composite parts have been utilized in FMLs. Liu and Liaw (2010) and Seyed Yaghoubi et al. (2012) have shown that FMLs with a cross-plied lay-up perform better under impact loading. The stacking [0˚/90˚/90˚/0˚] has been used most extensively. Recently, Seyed Yaghoubi et al. (2012) applied a quasi-isotropic stacking and found out a more condensed damage area after a low-velocity impact when compared to specimens with a unidirectional or cross-ply stacking.

Glass fibres have been known to outperform other common fibre materials in FMLs, as the high ultimate strain provides a postponed fibre failure for the structure. Vlot and Krull (1997) also concluded that the strain rate strengthening of glass fibres is one of the reasons for the high impact resistance of glass fibre based FMLs. For metal layers in general, the area under the tensile stress-strain curve prior to metal fracture has been stated to be a measure for the impact resistance and energy absorption capability (Vlot, 1991; Sadighi et al., 2012). In the current literature, the impact performance of different FML concepts based on aluminium, titanium, magnesium and steel layers have been studied (e.g. Vlot, 1996; Bernhardt et al., 2007; Cortes and Cantwell, 2005; Düring et al., 2015). Taking the hybridization of FMLs even further, Sarlin et al. (2014) and Düring et al. (2015) have recently introduced rubber layers into the metal-composite hybrid concepts.

Another vital purpose of the experimental low-velocity impact studies has been to solve the effects of geometrical parameters on the impact response. The scaling effects of certain testing arrangements have been studied by Carrillo and Cantwell (2008) and Mckown et al. (2008). The results of the normalized contact force–central deflection curves with different scaling factors showed good agreement, and the FMLs were determined to follow the simple scaling law. The effect of the specimen support shape on the impact response and damage characteristics has been approached by Vlot (1991) and Laliberté et al. (2005), who used rectangular and circular test areas for the specimens. The rectangular specimens showed major deformations at corners that were lacking in circular specimens. The effect of impactor shape on impact response and damage formation has been surveyed by Liu et al. (2014). The smaller impactor was shown to cause more severe local damages in Glare FMLs. In addition, Morinière (2014) recently extended the classical approach of a single impact to the centre of the specimen by studying the effects of repeated impacts and off-centre located impacts on the load response and damage characteristics.

The impact loading on FMLs is simulated either by using analytical models or numerically solved finite element (FE) models in the relevant literature. Vlot (1991) introduced the first analytical impact model for FML structures to study the effects of low-velocity impact loading. The model was capable of capturing the elastic-plastic response of metal layers. Later on, other theoretical approaches have been introduced (Lin and Hoo Fatt, 2006; Tsamasphyros and Bikakis, 2011; Payeganeh et al., 2010). Most recently, Morinière (2014) compiled an analytical model to study low-velocity impact loading on FMLs. Delamination and debonding damage were also included in the model. Laliberté (2002) was the first to comprehensively model FMLs under low-velocity impact by means of FE modelling. Since then, several FE analyses have been performed to dissect the impact response (see Section 4.1.3). The development in the modelling is summed up in recent review articles by Chai and Manikandan (2014) and Morinière et al. (2014).

## 2.2 Debonding

In the current literature, the initiation of low-velocity impact damaging of FMLs has been discussed to be due to the local plastic deformation of the metal at the impact point (Laliberté, 2002). During the early phase of the loading, delamination and debonding together with matrix cracking are also described as taking place due to shear forces (Vlot, 1991; Laliberté, 2002). Finally, when the ultimate strain is locally exceeded in the fibres and metal, fibre fractures and metal cracking occur. Depending on the level of the impact energy with respect to the panel's impact response, the impactor rebound may occur and the accumulated elastic strain energy of the panel tends to transform back into the impactor kinetic energy. If the impact energy is high enough, the perforation of the panel occurs, and consequently fibre fractures and metal cracking extend.

The energy absorption capabilities of various impact damage modes in FML structures are uneven. Strong damage modes (i.e. metal plastic deformation, fibre failures and metal cracking) absorb most of the impact energy and also strongly control the contact force–central deflection response of the FML (Laliberté, 2002; Hagenbeek, 2001; Morinière et al. 2014). Therefore, many of the impact damage models developed in the relevant literature have primarily focused on taking the strong damage modes into account. Setting a perspective for the energy absorption capabilities of weaker damage modes, Morinière et al. (2013) concluded that, at maximum, 7.6% of the FML's absorbed energy was consumed by the delamination and debonding in small Glare specimens. The energy absorption by delamination and debonding for larger specimens was zero or close to zero. In their analytical model, Morinière et al. assumed pure shearing fracture mode II crack tip loading for the debonding and delamination, and the fractures were assumed to occur instantly at a certain critical contact force.

Laliberté (2002) was the first to develop finite element models for the debonding in FMLs under low-velocity impact loading. The models were based on explicit time integration and the simulations were performed by using LS-DYNA (LSTC). The layers of Glare FMLs were modelled with thick-shell elements and different variations of tiebreak contact were used to simulate the debonding in Glare FML panels. The failure of the tiebreak contact was assumed to occur under the following failure criterion

$$\left(\frac{|\sigma_n|}{NFLS}\right)^2 + \left(\frac{|\sigma_s|}{SFLS}\right)^2 \geq 1 \tag{2.1}$$

where $\sigma_n$ is the normal stress at the interface, $\sigma_s$ is the shear stress at the interface, $NFLS$ is the tensile failure strength of the interface and $SFLS$ is the shear failure strength of the interface. The results showed a broad debond for all the studied panels at the upper aluminium and glass fibre reinforced layers' interface after the simulated loading. The share of fracture mode I (peeling) on the debond crack tip propagation was already established, although fundamental conclusions for such propagation of debonding were missing.

Nakatani et al. (2011) studied low-velocity impacts on titanium and glass fibre/epoxy FMLs (Ti/GFRP) by using an FE model generated using Abaqus/Explicit (Dassault Systèmes). The titanium layers in their FMLs were simulated using solid elements and the composite layers using shell elements. Debonding at the lower titanium-glass fibre/epoxy interface was assumed to occur at a certain instant during the loading step. The debonding was taken into account in the model by manually releasing related nodal contacts at the interface during the impact loading. They concluded that if metal cracking did not occur, the debonding resulted in a broader damage area when compared to delamination, i.e. the debond controlled the extension of interfacial damaging in the panel.

Tsartsaris et al. (2011) used an explicit finite element code LS-DYNA and shell elements for studying the low-velocity impact response of aluminium-glass fibre/epoxy FMLs. Fibre fracture and matrix cracking, as well as debonding and delamination models, were included in the FML simulation. Debonding was modelled by using tiebreak contacts. The model included a bilinear traction-separation law (Fig. 2.1) with a mixed-mode damage criterion.

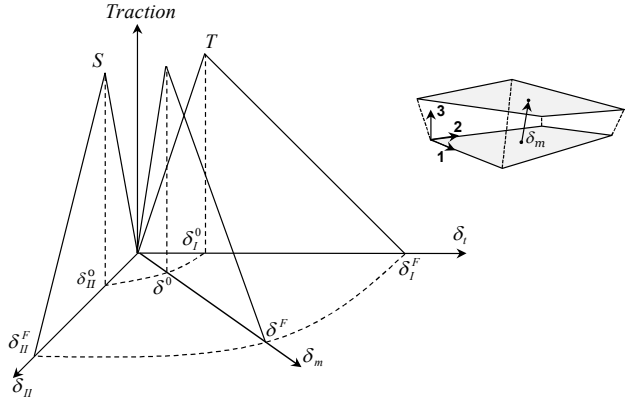


**Figure 2.1.** Cohesive material model used in the study of Tsartsaris et al. (2011).

The mixed-mode displacement was calculated from the single-mode displacements as follows

$$\delta_m = \sqrt{{\delta_I}^2 + {\delta_{II}}^2} \tag{2.2}$$

where the separation in the normal direction of the plane $\delta_I = \delta_3$ and the separation in the tangential direction of the plane $\delta_{II} = \sqrt{{\delta_1}^2 + {\delta_2}^2}$, see Fig. 2.1. The mixed-mode damage initiation displacement $\delta^0$ was defined as

$$\delta^0 = \delta_I^0 \delta_{II}^0 \sqrt{\frac{1+\beta^2}{(\delta_{II}^0)^2 + (\beta\delta_I^0)^2}} \tag{2.3}$$

where $\delta_I^0 = T/EN$ and $\delta_{II}^0 = S/ET$ are single-mode damage initiation separations, $T$ and $S$ are the peak tractions in normal and tangential directions, $EN$ is the stiffness normal to the interface, $ET$ is the stiffness tangential to the interface and $\beta = \delta_{II}/\delta_I$ is the mode mixity. The ultimate mixed-mode displacement $\delta^F$ representing the total failure was defined according to the Benzeggagh-Kenane law

$$\delta^F = \frac{2}{\delta^0\left(\frac{1}{1+\beta^2}EN + \frac{\beta^2}{1+\beta^2}ET\right)} \cdot \left(G_{IC} + (G_{IIC} - G_{IC})\left(\frac{\beta^2 ET}{EN + \beta^2 ET}\right)^{|XMU|}\right) \tag{2.4}$$

where $XMU$ is the exponent of the mixed-mode criterion, $G_{IC}$ is the Mode I critical strain energy release rate and $G_{IIC}$ is the Mode II critical strain energy release rate. The simulations indicated that debond was present especially at the lowest interface between the aluminium and glass fibre reinforced layer.

The information about the debonding during low-velocity impacts provided by the current literature is still somewhat unclear. Many of the models taking into account the debonding presumed only shearing loads for the crack tip (fracture mode II). Some of the studies, on the other hand, have suggested peeling load (fracture mode I) participation in the debonding. Airoldi et al. (2009) studied the debonding in quasi-static indentation-loaded FML panels with a finite element model (Abaqus/Explicit) and by using cohesive elements. The cohesive model was based on a bilinear traction-separation law. The results revealed the debonding in type 2/1 aluminium-glass fibre/epoxy laminates during the loading phase (upper interface) and the unloading phase (lower interface). The debonding at the upper interface was suggested to be a result of shearing loads. The lower interface debonding in turn was suggested to be a result of peeling loads.

# 3. Materials and methods

## 3.1 Materials

In total, four types of FMLs were applied in the research. In Part I (P1, P2), magnesium and aluminium-based glass fibre-epoxy laminates with type 3/2 stacking were utilized (Fig. 3.1). In Part II (P3, P4), stainless steel based FMLs with carbon fibre-epoxy and glass fibre-epoxy layers were prepared. Additional adhesive layers were applied between the steel sheets and composite parts. The following materials were used in the research:

- Magnesium alloy: AZ31B-H24 (Magnesium Elektron)
- Aluminium alloy: 2024-T3 (Alcoa)
- Stainless steel alloy: AISI 304L (Outokumpu)
- Unidirectional prepreg: S2 glass fibres impregnated in FM94 epoxy adhesive (Cytec)
- Unidirectional prepreg: T700 carbon fibres impregnated in M21 epoxy resin (Cytec)
- Adhesive film: FM 300NK (Cytec)
- Adhesive film: FM 300-2 (Cytec)

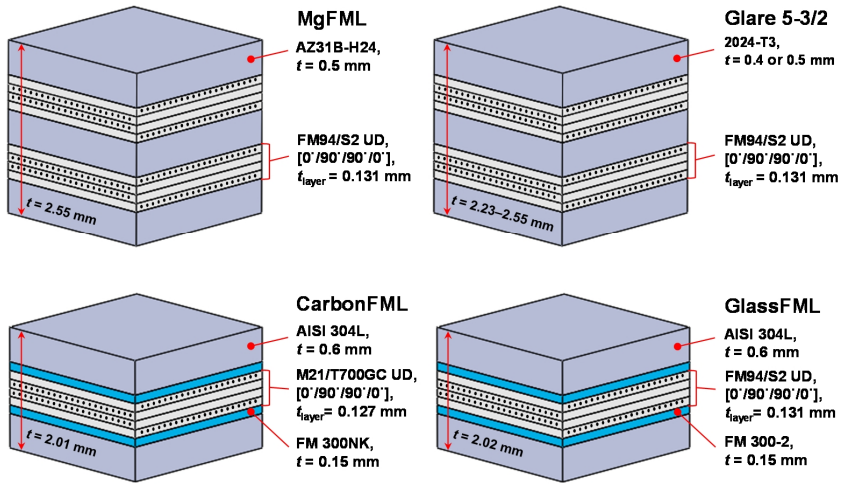


**Figure 3.1.** Schematics of the FMLs studied in this thesis. MgFML and Glare 5-3/2 laminates were used in Part I (P1, P2), whereas CarbonFML and GlassFML were exploited in Part II (P3, P4). Layer thicknesses are not in scale.

One purpose of Part I was to study how the tensile stress-strain response relates to the impact resistance of FMLs. Therefore, two laminates containing different metal alloys were needed in the experiments. The selection of aluminium alloy (2024-T3) was natural as it is widely used in FMLs. Magnesium on the other hand is the lightest structural metal ($\rho_{mg}$ = 1.8 kg/dm$^3$ vs. $\rho_{al}$ = 2.8 kg/dm$^3$), which makes it a candidate for weight-optimized FML structures (e.g. for aerostructures). Alderliesten et al. (2008) concluded that AZ31B-H24 magnesium alloy possesses comparable density-normalized static properties with 2024-T3 aluminium alloy. Therefore, the alloy was selected to study its applicability in FMLs. While the direct comparison in material density shows disadvantage for steel alloys ($\rho_{steel}$ = 8.0 kg/dm$^3$), they are used in FMLs due to their high stiffness and high bearing strength (van Rooijen, 2006). Steel based FMLs with carbon FRP layers have been applied to structures with mechanical fastenings (Hühne and Petersen, 2014; Kolesnikov et al., 2013). Recently, Düring et al. (2015) have also studied applicability of a steel, rubber and carbon FRP hybrid for impact prone leading edges of airliners' wings. The main purpose for the usage of AISI 304L stainless steel in the research of this dissertation was the need for high ultimate strain metal in the laminates. The high ultimate strain was needed to postpone metal cracking as a function of impact energy and consequently to gain better focus on the debond damage mode.

## 3.2 Experimental methods

The low-velocity impact damaging was studied by using drop-weight impact and quasi-static indentation tests (Fig. 3.2). All the impact and indentation tests were based on the test geometry where a square test specimen (110 x 110 mm$^2$) was clamped between two steel fixtures with an 80 mm diameter circular test area. The loading of the specimens was carried out with a 15.9 mm diameter hemispherical contactor head. In total, 60 drop-weight impact specimens were tested in Part I, and 36 drop-weight impact and nine indentation specimens were tested in Part II.

The primary methods for the post-impact and post-indentation damage assessment of the specimens were the measurements of free surface profiles, ultrasonic scanning and analyses of the laminate cross-sectionals. The straining of the free surfaces was studied by using a 3-D digital image correlation method-based machinery as well as strain gauges.

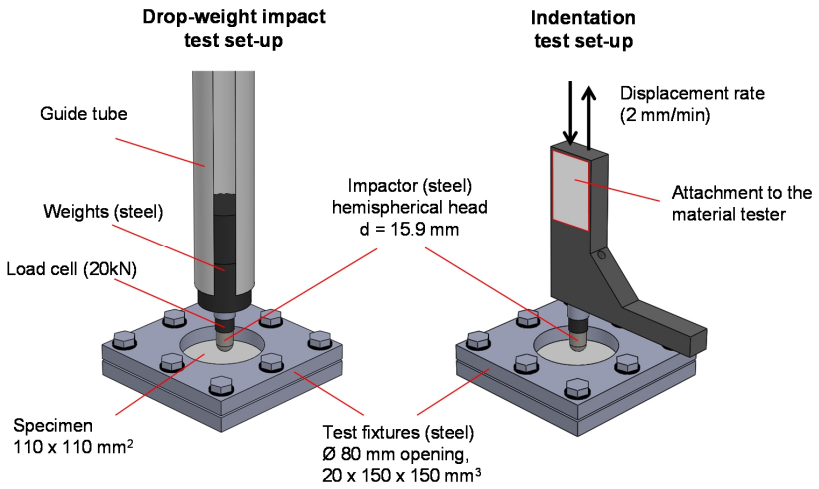


**Figure 3.2.** The drop-weight impact and quasi-static indentation test set-ups.

## 3.3 Modelling methods

The low-velocity impact simulations were performed using Abaqus finite element software (Dassault Systèmes). A dynamic non-linear transient model was developed by using Abaqus/Explicit in Part I to study the impact response of FMLs. The model included damage criteria for in-plane damages but neglected the debonding and delamination. The layers were modelled using either solid (C3D8R) or continuum shell elements (SC8R). The modelling is further introduced in Section 4.1.3.

The debonding of a low impact energy specimen was in focus in Part II. The impact model was based on the quasi-static loading assumption (Abaqus/Standard) and therefore ignored strain rate effects and wave propagation. A similar approach has been previously exploited in many low-velocity impact simulations (e.g. Vlot, 1991; Olsson, 2000; Chai and Manikandan, 2014). The models in Part II were built using solid elements (C3D8I).

The damage modelling in Part II took into account the plastic deformation of the steel sheets (Johnson-Cook model) and debonding but neglected other damage modes. Cohesive zone modelling (CZM) by cohesive elements (COH3D8) was utilized for the debonding and the failure was modelled by using a bilinear cohesive zone law. The debond initiation obeyed the following quadratic nominal stress criterion

$$\left(\frac{\langle t_n \rangle}{t_n^0}\right)^2 + \left(\frac{t_s}{t_s^0}\right)^2 + \left(\frac{t_t}{t_t^0}\right)^2 = 1 \qquad (3.1)$$

where $t_n$, $t_s$, $t_t$ are the tractions in the normal and two shear directions of the plane whereas $t_n^0$, $t_s^0$, $t_t^0$ are the corresponding critical tractions. The damage evolution followed a power law criterion

$$\left(\frac{G_n}{G_n^C}\right)^{\alpha} + \left(\frac{G_s}{G_s^C}\right)^{\alpha} + \left(\frac{G_t}{G_t^C}\right)^{\alpha} = 1 \tag{3.2}$$

where $G_n$, $G_s$, $G_t$ are strain energy release rates in the normal and two shear directions of the plane, and $G_n^C$, $G_s^C$, $G_t^C$ are the corresponding critical strain energy release rates. The exponent $\alpha = 1$ was used in the simulations.

It is important to be aware that debonding can also be studied with other modelling methods. Since the introduction of the cohesive zone approach (Dugdale, 1960; Barenblatt, 1962; Hillerborg, 1976), several cohesive zone laws have been developed (Needleman, 1987; Rice and Wang, 1989; Tvergaard and Hutchinson, 1992; Xu and Needleman, 1994; Camanho and Ortiz, 1996; Geubelle and Baylor, 1998; Blackman et al., 2003). These are classified to bilinear, trapezoidal, parabolic and exponential laws. Also, there exists a variety of damage initiation and damage evolution laws in the literature, e.g. the Benzeggagh-Kenane law (Benzeggagh and Kenane, 1996). When compared to the approach used in this study (i.e. bilinear model, quadratic nominal stress criterion and power law assumption), the methods may provide more accurate results. However, the applied simple approach was seen to describe well enough the overall debonding mechanisms, which are in focus of the thesis, and was therefore chosen for the simulations. It should also be noted that, in addition to the standard finite element method, the extended finite element method (XFEM) has proven to be efficient in modelling of damages in structures, and could be applied for FMLs to study detailed damage mechanisms during impact loading (Moës et al., 1999; Curiel Sosa and Karapurath, 2012).

# 4. Results and discussion

## 4.1 Part I – Impact resistance, impact damage process and impact response of FMLs (P1, P2)

### 4.1.1 The influence of metal layers on impact resistance

The research was started by studying the influence of metal layers on the impact resistance of FMLs (P1, P2). As an engineering objective, the applicability of AZ31B-H24 magnesium alloy for FMLs was studied by comparing the impact response of magnesium alloy-based FML specimens (MgFML) with 2024-T3 aluminium alloy-based Glare FMLs (Glare 5-3/2-0.4 and Glare 5-3/2-0.5). The impact performance of aluminium and magnesium-alloy based FMLs has previously been compared by Cortes and Cantwell (2005) as they studied 2024-O and AZ31 alloys for FMLs. In their research, a magnesium-based structure was shown to have a higher impact resistance against perforation.

The fracture process of FMLs under impact loading is dependent on several macroscopic factors, for example the thickness and stiffness properties of the panel. Therefore, two comparison methods were applied: the equal thickness approach and the equal bending stiffness approach. The idea behind the equal thickness approach is that the thickness of the metal layers in the specimens under comparison is the same, and consequently the thickness of the specimens is equal (MgFML and Glare 5-3/2-0.5). However, the stiffness properties of AZ31B-H24 and 2024-T3 are not equal, and the bending response of the equal thickness specimens differs. Therefore, thinner aluminium layers were applied for the Glare specimens in the equal bending stiffness approach, i.e. the thickness of aluminium layers in Glare specimens was chosen so that the bending stiffness closely responded to that of the MgFML specimens (MgFML and Glare 5-3/2-0.4).

First cracking, second cracking, and perforation limits were studied in the research (P1). Here, the first cracking limit refers to the impact energy needed to form a first visually detectable crack in the surface metal layer, the second cracking limit refers to the energy needed to form a crack in both surface layers, and the perforation limit refers to the energy needed to fully perforate the specimen. The impact performance was further studied by comparing specific impact energies, i.e. limit energies divided by the areal densities of the specimens. The results (Fig. 4.1) did not show an advantage for the MgFML specimens as the

specific first cracking limit was 305–333% higher and the specific second cracking limit was 113–122% higher for the traditional Glare 5 panels. The specific perforation limits of the MgFML and Glare 5 panels were on the same level.

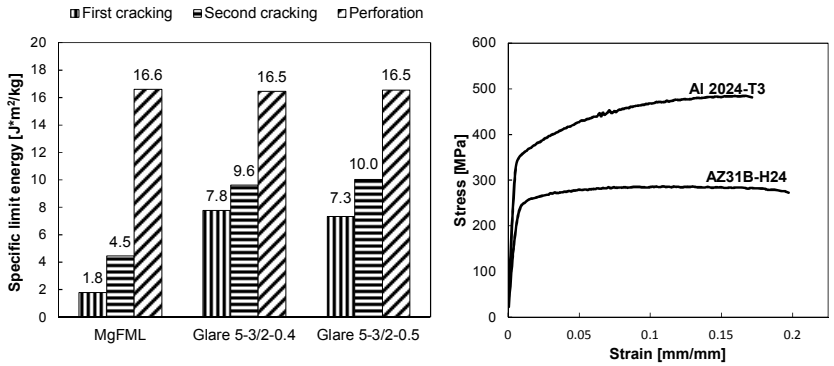


**Figure 4.1.** The specific limit energies for MgFML and Glare 5 specimens determined by experiments, and the experimental tensile stress-strain curves for AZ31B-H24 magnesium and 2024-T3 aluminium alloys in the rolling direction.

The research also provided a way to examine the effect of metal stress-strain response on the impact resistance. Previously, Vlot (1991) has discussed that the area under the tensile stress-strain curve represents the capability of a metal alloy to absorb energy during an impact and therefore contributes to the impact resistance of a metal layer or FML panel. However, the area under the stress-strain curve of AZ31B-H24 compared to the area of 2024-T3 cannot explicitly explain the difference in the specific first and second cracking energies between the MgFML and the Glare FMLs (see Fig. 4.1). The area of 2024-T3 under the stress-strain curve is 47% higher when compared to AZ31B-H24 (rolling direction); the difference is significantly less when compared to the measured specific first and second cracking energy differences.

Metal layers crack under impact loading when they *locally* reach the ultimate strain of the material. Impact loading generates a zone of high strain close to the impact point (further discussed in Section 4.2.5). The zone of high strain is expected since the load bearing capability of a panel increases along with the increasing distance away from the impactor contact point. Thus, impact loading will make the radial straining uneven over the test area – even for isotropic and linear-elastic materials. As an elastic-plastic material is involved here, the plastic deformation will further weaken the load transfer from the impact point and intensify strain peaking at the impact point.

AZ31B-H24 was determined to have a negligible rate of strain hardening at the plastic zone (Fig. 4.1). Therefore, it is apparent that after the magnesium layers in the MgFML locally reached the yield limit at the impact point, the load-transfer towards the clamped boundaries significantly decreased. As a result, the strains accumulated near the impact point – resulting in premature cracking. The strain hardening rate for 2024-T3 was higher and therefore the Glare

panels transferred loading more efficiently away from the impact point. As a result, the area around the impact point absorbed a higher amount of impact energy and the local peak strain at the impact point was lower than for the MgFML. For this reason also the first and second cracking limits of the Glare panels were expected (and observed) to be higher. It seems that a high strain hardening rate of a metal is desirable when a high impact resistance (for metal cracking) in FMLs is desired. Detailed studies are needed, however, to further quantify the phenomenon and to verify its significance.

### 4.1.2 Impact damage characterization of aluminium and magnesium alloy-based FMLs

The damage evolution and post-impact damage patterns in the MgFML and Glare 5 specimens were studied in P1. The first visual sign of impact damage was the plastic deformation of the metal layers, i.e. a dent under the impact point. As the targeted impact energy (and consequently the dent size) was increased per specimen series, the first visible crack formed in the back wall metal sheet. Along with the increased impact energy, visible cracks formed on the surface of the impact side metal sheet and, finally, the full perforation occurred. The post-impact cross-sectionals revealed that the inner metal sheets cracked at impact energies between the first and second cracking energy limits.

Similar types of damage patterns for metal layers in FMLs have been previously reported in the current literature. Morinière et al. (2013) simulated the behaviour of a Glare 5-2/1 laminate. According to the simulation results, the metal layers became plastically deformed at an early stage of the impact event and a dent formed. The metal cracking occurred first in the lower metal sheet, after which cracking of the impacted side followed. Caprino et al. (2004) experimentally studied FMLs with three aluminium layers. The impact energy limit for the cracking of the central aluminium layer occurred between the energy levels needed to crack the upper and lower aluminium sheets. Laliberté (2002) observed similar behaviour for the aluminium layers in Glare panels but also found that the fibre alignment and the amount of fibres in specific directions affect the metal crack patterns. The cracks formed equally in the laminate's 0° and 90° directions when there was an equal amount of fibres in these directions. When the fibre fraction was 67/33 in the 0° and 90° directions, the crack in the bottom aluminium layer formed only in the controlling 0° fibre direction.

The post-impact cross-sectional images and ultrasonic inspections in P1 further explained the damaging process inside the FMLs. At a low impact energy (20 J), prior to extensive fibre failures, the cross-sectionals of the MgFML and Glare 5 specimens revealed a debond at the interface next to the back wall metal sheet (Fig. 4.2a). Delaminations inside both composite parts were mainly formed at 0°/90° composite layer interfaces closest to the impact side. These damage patterns were consistent for the MgFML and Glare 5 specimens.

Many of the cross-sectional studies in the current literature for impacted cross-plied FMLs have proved that the highest opening between the layers (debonding) occurs at the interface between the lowermost metal layer and the rest of the laminate (Wu and Yang, 2005; Fan et al., 2011a; Nakatani et al., 2011; Seyed Yaghoubi et al., 2012; Yarmohammad Tooski et al., 2013). The cross-sectional studies reported in the current literature have also shown that debonds or delaminations are present at other interfaces as well, but the patterns are not consistent, i.e. they are clearly more dependent on the specific laminate structure and materials.

Both cross-sectional images and ultrasonic C-scans in P1 revealed debond and delamination in the MgFML and Glare 5 specimens already prior to the metal cracking and extensive fibre fractures, which were visible in the cross-sectional images for the high impact energy specimens (Fig. 4.2b). The values of total damage size, i.e. the combination of debond and delamination in the MgFML and Glare 5 specimens without metal cracking, were small and focused close to the impact point. However, when the metal cracking occurred, the C-scans revealed large damage surrounding the metal cracks (Fig. 4.2b). The through-transmission ultrasonic inspection (UI) reveals the debonded and/or delaminated area and cannot sort out whether the damage generates around the metal cracks in the form of debond or delamination. Either way, a high ductility AISI 304L stainless steel was chosen for the debonding studies of Part II in order to postpone metal cracking and, consequently, to simplify the damage process and to emphasize the role of the debonding.

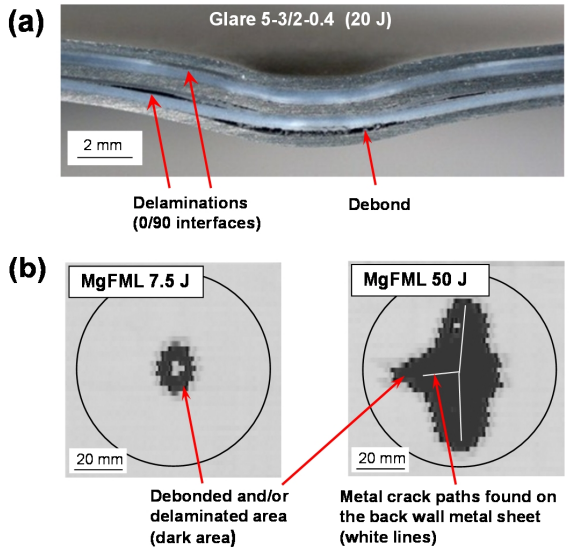


**Figure 4.2.** Damage characterization in P1: (a) typical debond and delamination damages found in the cross-sectional study of low impact energy (20 J) specimens and (b) the total damage area measured by UI in a specimen without metal cracking and in a specimen with metal cracks in the back wall metal sheet.

### 4.1.3 Impact modelling

Analytical models are efficient for parametrical studies when modelling the impact on FMLs. However, finite element modelling is capable of capturing material and geometrical non-linearity better than analytical models (Morinière, 2014). Therefore, an attempt to model the impact response of FMLs by means of finite element modelling was carried out in P2. Rather than focusing on the development of an accurate model which takes into account all possible damage modes, the primary aim of the work was to make a rough dynamic non-linear transient model with Abaqus to study the impact response. The modelling part of P2 was carried out by the co-authors Sayeaftabi and Sadighi and the results of the performed simulations work as a background information for the impact modelling of Part II.

The modelling was based on the existing models for FMLs found from the current literature (Guan et al., 2009; Song et al., 2010; Seo et al., 2010). The main differences in these models are the type of chosen elements, mechanical behaviour description and damage criteria selection for the constituents of the FML. Guan et al. (2009) used 8-node solid elements for both metal and composite layers. The metal was modelled as an elastic-plastic material with a rate dependent response, whereas the composite part was modelled as an isotropic material. The failure criterion of the metal layers included tensile and shear stress components. A tensile failure criterion was applied for the composite layers. Song et al. (2010) utilized 8-node solid elements for the metal layers and 8-node continuum shell elements for the composite layers. The metal and composite layers were modelled as isotropic and orthotropic materials, respectively. Hashin's damage criterion, which takes into account tensile, compressive and shear stress components, was applied for the composite layers. The metal layers had no damage criterion since it was expected that no damage occurs during the loading. Seo et al. (2010) formed two models in which the composite layers were modelled either using 8-node solid or 8-node continuum shell elements with an orthotropic material model. The metal layers were modelled by 8-node solid elements with an isotropic linear-elastic response. Since the Hashin's damage model in Abaqus is not applicable for solid elements, a user-defined Hashin's 3D criterion was implemented. The metal layers did not have any damage criterion. Damage models for the debonding and delamination were not implemented in any of these models.

Two different modelling methods based on the above-mentioned models were adopted in P2 with some specific advances (see Table 4.1). The metal layers in both models used 8-node solid elements (C3D8R) and were modelled as an isotropic elastic-plastic material with rate dependent material properties. The damage process in the metal layers was modelled by using shear and tensile stress/strain failure criterion. The composite part in the first model followed the approach of Guan et al. (2009) with the use of 8-node solid elements. In addition, the composites utilized an isotropic material model with a damage criterion for tensile stress/strain. The second model applied the approach of Song et

al. (2010) for the composite part: 8-node continuum shell elements (SC8R) and an orthotropic material model with the Hashin's damage criterion were used. Debonding and delamination were not implemented in these models since the main emphasis was to study the effect of element type (and failure criteria) on the simulated impact response.

**Table 4.1.** Essential features of the finite element models in P2.

| Model | Metal layers | Composite layers | Metal layer failure | Composite layer failure |
|---|---|---|---|---|
| Model 1 | Solid elements, isotropic elastic-plastic model | Solid elements, isotropic linear-elastic model | Max tensile and shear stress | Max tensile and shear stress |
| Model 2 | Solid elements, isotropic elastic-plastic model | Solid-shell elements, ortotropic linear-elastic model | Max tensile and shear stress | Hashin's damage criterion |

The impact response of the MgFML and Glare 5 specimens with impact energies ranging from 30 J to 80 J were simulated using the first model (model 1, solid elements for the composite parts). The largest error in the predicted maximum contact force, when compared to the experimental results, was about 12% and was found for the MgFML specimen loaded by an 80 J impact (Fig. 4.3a). Also, simulation results provided by the first and second models were compared with the experimental result of a Glare 5-3/2-0.4 specimen loaded by a 30 J impact (Fig. 4.3b). The impact response of the model 2 (continuum shell elements for the composite parts) included several damage indications, i.e. discrete load drops, which were not observable from the experimental results. Also, the impact response of the model 2 resulted in a steeper load-increase with higher contact force values and, finally, over a 20% difference in the maximum contact force when compared to the experimental results. The growth of the contact force and the maximum contact force resulting from the model 1 were in better agreement with the experimental results compared to model 2.

Seo et al. (2010) obtained somewhat similar results when they studied the impact response of FMLs using two different models – one with continuum shell elements plus Hashin's 2D damage criterion for the composite layers, and another with solid elements and Hashin's 3D damage criterion for the composite layers. The results of both simulations showed good agreement with test results of specimens having a barely visible impact damage (BVID) and with test results of specimens having clearly visible impact damage (CVID). In terms of the peak impact force and permanent displacement, the three-dimensional approach led to more accurate results.

Since the modelling work of P2, new approaches to study low-velocity impact response of FMLs by means of finite element modelling have been introduced (Fan et al., 2011b; Nakatani et al., 2011; Tsartsaris et al., 2011; Zhu and Chai, 2012; Liu et al., 2014; Zhou et al., 2014; Yu et al., 2015; Asaee and Taheri, 2016). Many of these studies have focused on advancing the in-plane damage models.

Continuum shell elements and solid elements have been applied for the composite layers, although solid elements have been preferred in the latest models. The next step for advancing the models of FMLs is to accurately take the debonding and delamination into account. Since these damages are governed by the out-of-plane loading of the adjacent layers, the incorporation of all stress/strain tensor components is needed for accurate damage representation (Seo et al., 2010).

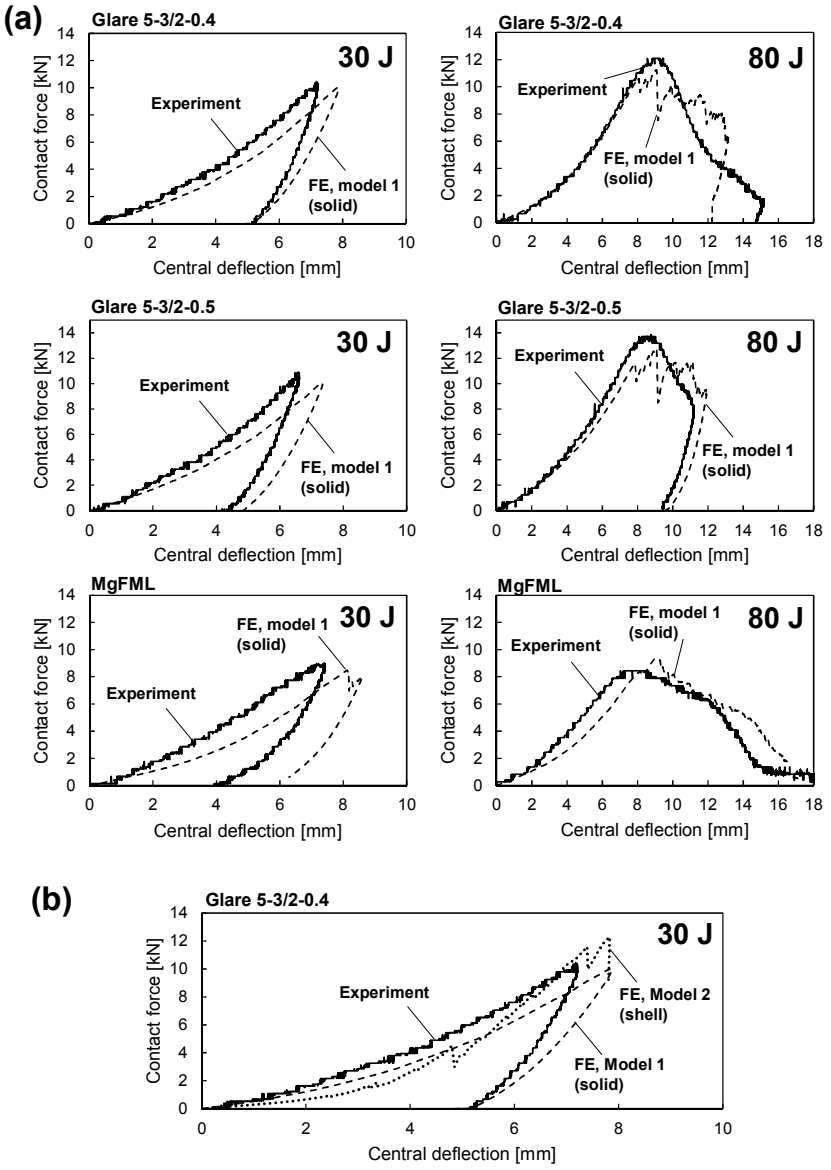


**Figure 4.3.** The contact force–central deflection curves determined by the experiments and FE simulations: (a) the results for Glare 5-3/2-0.4, Glare 5-3/2-0.5 and MgFML; (b) the results for Glare 5-3/2-0.4 (simulation results based on two different modelling approaches).

## 4.2 Part II – Debonding (P3, P4)

### 4.2.1 Impact damage characterization of steel based FMLs

In Part II, the laminate structure was simplified from type 3/2 stacking to 2/1 stacking, and the metal layers were replaced with AISI 304L layers in order to postpone metal cracking as a function of impact energy. Two laminate structures with different FRP layers were tested and analysed (CarbonFML and GlassFML).

First, drop-weight impact tests were performed within a selected impact energy range (5–94 J) to dissect the overall impact response in P3. The low impact energy specimens (10 J) without any (obvious) fibre fractures were further analysed to study the debonding and debond characteristics. Cross-sectional imaging, surface imaging and ultrasonic C-scans were utilized in the post-impact damage assessment. Contrary to the existing literature, the cross-sectionals were analysed in two directions instead of one, i.e. the cross-sections of a quarter specimen were analysed. The analysis is important because the final damage pattern is dependent on the lay-up of the studied cross-section.

Cross-sectionals are typically prepared by cutting the specimens along the mid-line directly after an impact event and then by polishing the cross-section surface of the sample piece. However, especially FMLs have high internal stresses after an impact loading, and the direct cross-sectional cutting may release a certain amount of stresses and consequently change the damage patterns (Laliberté et al., 2005). In addition, the cutting itself causes mechanical loading and result in further damaging – especially at the metal-adhesive interface. In order to minimize the changes in the damage patterns, the steel layers were chemically dissolved away prior to the cutting. Also, the dissolution allowed direct characterization of the debond fracture surface inside the laminate without any mechanical sample preparations. Therefore, the adhesive and the composite part of the specimen were analysed in our cross-sectional study. The scanning electron microscopy imaging was performed for the specimens after dissolving the metal layers, i.e. the surfaces of the adhesive films were analysed. The aim was to characterize the details of debonds from the fracture surfaces.

The post-impact damage assessment study revealed debonds in both types of specimens (CarbonFML and GlassFML) between the lower steel sheet and the composite part (Fig. 4.4). Debonds were found to exist either at the interface between the steel sheet and the adhesive film (for GlassFML) or inside the adhesive film (for CarbonFML). Additionally, the cross-sectional of the CarbonFML showed debond inside the upper adhesive film, i.e. cohesive failure had occurred. The analyses of the GlassFML specimen did not offer reliable information to judge whether or not the debonding occurred at the upper interface. Other types of damages found in the specimens were matrix shear cracks and delaminations of short length in the composite. The short delaminations ap-

peared in the longitudinal cross-sections at the interfaces between 0°/90°-composite layers, and they were connected to the shear cracks crossing through the central composite layers. The composite damage has been observed to initiate by shear cracking and the cracks are further connected to delaminations in the current literature (Richardson and Wisheart, 1996). In the transverse cross-sections, both FMLs showed delamination damage at the upper 0°/90° composite interface, and the delamination damage reached the upper adhesive film by shear cracks. The debonding was the controlling damage mode in both laminates, i.e. debond extended furthest away from the impact point.

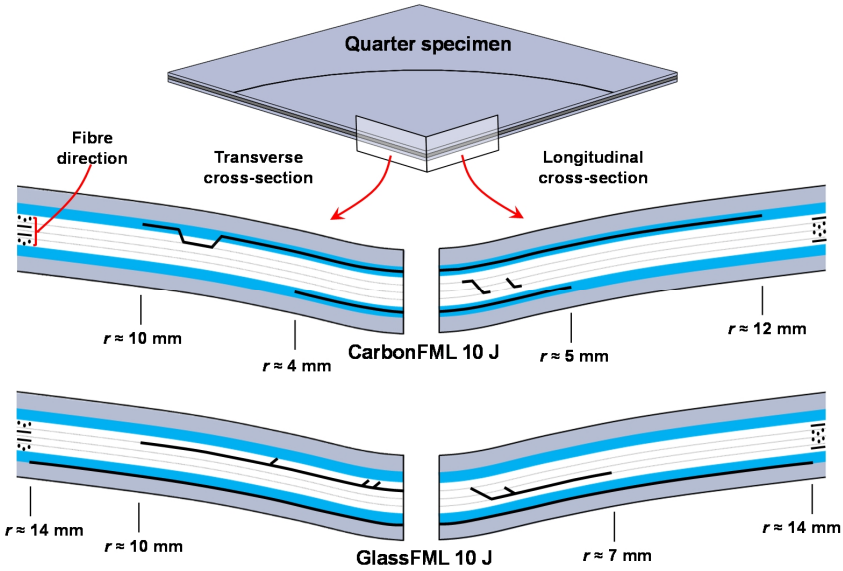


**Figure 4.4.** The post-impact damages found in CarbonFML and GlassFML specimens after the 10 J low-energy impact events. Note: The results could not explicitly show whether the debonding occurred at the upper interface of the GlassFML specimen.

For all the tested laminates in Part I and Part II, a common damage type was the debond between the lowermost metal sheet and the rest of the laminate. Supporting the generality of our finding, the debond at the lowermost interface is also found in several post-impact cross-sectionals in the relevant literature (as discussed in Section 4.1.2) – especially for [0°/90°/90°/0°] cross-plied FMLs.

### 4.2.2 Debond fracture surface characterization

Debond characteristics were further studied in P3. The debond characteristics were studied by analysing the GlassFML (10 J) specimen, i.e. the fracture surface morphology of the lower side adhesive film after the dissolution of steel sheets was examined (Fig. 4.5). The fracture surface around the impact point ($5 < r < 6$ mm) contained striations and torn shreds of adhesive. These signs are typical for fracture surfaces, which have failed under pure shearing crack tip loading (fracture mode II) (Burianek and Spearing, 2004). However, the

debond area had extended further and the adhesive surface ($r$ > 6 mm) resembled the morphology of the steel sheet prior to bonding. The surface included ridges that corresponded to the grain boundary grooves found from the surface of the as-received steel sheet. The region of ridges suggested a dominance of a peeling load at the crack tip during the debonding (fracture mode I).

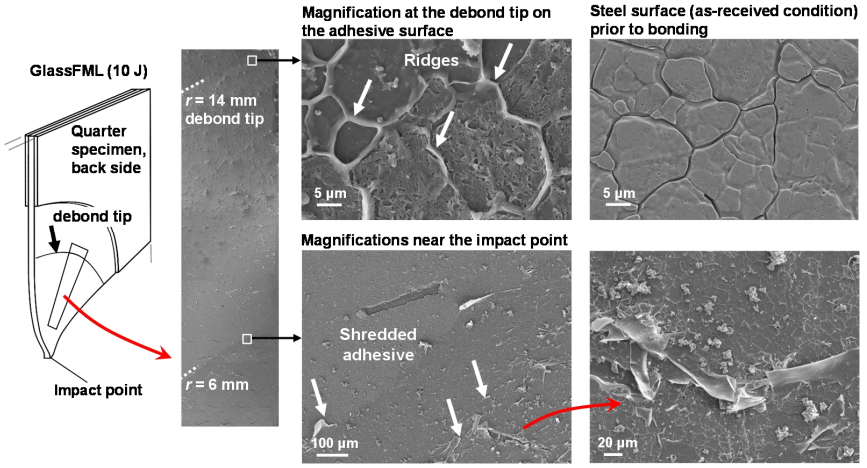


**Figure 4.5.** The post-impact surface images on the lower adhesive film of the GlassFML (10 J) specimen after the dissolution of steel sheets. The area around the impact point (5 < $r$ < 6 mm) contained striations and torn shreds, which suggests shearing crack tip loading for the debond. The area outside ($r$ > 6 mm) resembled the surface morphology of the steel sheet prior to bonding (upper right). This type of morphology suggests the dominance of peeling load at the crack tip.

The shearing load at the metal-composite interfaces is expected because out-of-plane shear loads are generated during the impact. However, the peeling loads causing fracture mode I -dominated debonding were considered to be generated during the rebound of the impactor (see Fig. 4.6). When the rebound phase of the impact event begins, each metal layer has a plastically deformed shape and, after releasing the elastic portion of the strain energy, they tend to preserve the deformed shape. The composite layers, on the other hand, will behave as a linear-elastic material (if any massive fibre fractures have not occurred); they tend to straighten until the end of the impactor contact. This discrepancy in the material behaviour will generate peeling loads at the interfaces and the debond will propagate if the critical strain energy release rate (SERR) limit at the crack tip is exceeded.

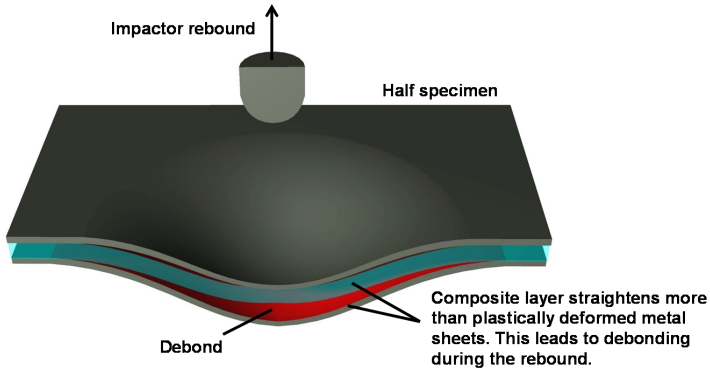


**Figure 4.6.** The discrepancy in material response between the metal and composite layers will generate peeling forces in the interface between the lower metal sheet and composite part during the rebound. The peeling forces lead to debonding if the critical SERR value is exceeded.

### 4.2.3 Modelling of debonding

Finite element simulations were performed to further explain the debonding in FMLs. The CarbonFML (10 J) specimen was chosen as a reference for the simulations for two reasons. First, we had clear information on the post-impact debond patterns. Second, debonding was clearly the dominating damage mode in the CarbonFML specimen, and therefore the influences of other damage modes (matrix cracking and delamination) on the impact behaviour were small (see Fig. 4.4).

Our background study for the debonding modelling has been recently published (Pärnänen et al., 2015). In this background study, the debonding was modelled only at the lower steel-composite interface. In order to simplify the system, debonding was modelled to occur at the interface of the steel sheet and adhesive. First, the virtual crack closure technique (VCCT) (Rybicki and Kanninen, 1977; Raju, 1987; Krueger, 2004) was applied for observing strain energy release rate (SERR) values per each of the fracture modes at a non-growing debond crack tip during the impact loading. The simulations were performed using circular pre-cracks of different sizes to represent initial debond. The results showed pure fracture mode II strain energy release rates (SERR) at the debond crack tip for the loading step of the impact event (Fig. 4.7). As the unloading step followed, the mode II values decreased. On the contrary, fracture mode I SERR values were initially zero during the loading step. However, the values suddenly increased during the end part of the unloading step, reaching the critical SERR level for certain pre-crack sizes. Therefore, the results suggest that the crack-tip of the debond is loaded by mode II during the loading step, whereas a mixed-mode loading with a peeling load dominance emerges at the crack tip during the end part of the unloading step.

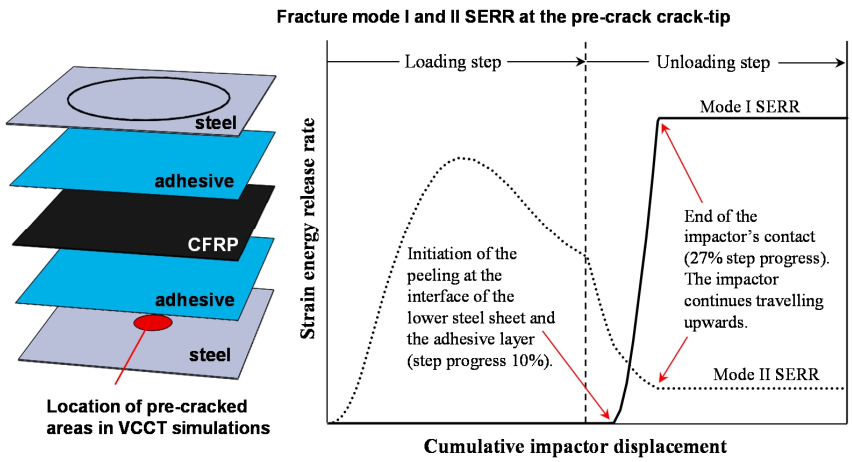


**Figure 4.7.** Schematics of the SERR values at the crack tip of the pre-crack (debond) during the impact loading of a simulated CarbonFML specimen. (Pärnänen et al., 2015)

Additionally, the debonding at the lower steel-adhesive film interface was also studied using the CZM method (Pärnänen et al., 2015). Various material properties for the cohesive damage law were used in the models in order to study the sensitivity of the CZM and the debonding on these properties. The results were similar to the VCCT results as the debond tended to initiate and grow during the early part of the loading step. Independent of the material properties, the damage further extended during the final part of the unloading step forming a circular shaped debond by the end of the contact ($r$ = 3.9–4.8 mm).

In P3, the cross-sectionals of the CarbonFML (10 J) specimen revealed debonding also inside the upper adhesive film (Fig. 4.4). Therefore, the modelling work was advanced in P4 by taking into account the debonding also at the interface of the upper steel sheet and adhesive film. The numerical modelling was implemented by applying zero-thickness cohesive elements along the upper and lower steel-adhesive interfaces. The material properties for the damage law were chosen from our background study (Pärnänen et al., 2015) and these values resulted in the highest (conservative) resistance to debond initiation.

The results of P4 revealed that the debond at the upper interface tended to grow more extensively during the loading step when compared to the lower interface (Fig. 4.8). The debond at the upper interface arose during the early part of the loading step and continued to evolve until the end of the step. The debond did not grow further as the unloading step progressed. The lower interface, on the other hand, did not show any apparent debonding during the loading step. However, a debond emerged during the end part of the unloading step and a circular debond had formed by the end of the impact. The size of the debond was close to the debond size found in our background study (Pärnänen et al., 2015) modelled with equal material parameters.

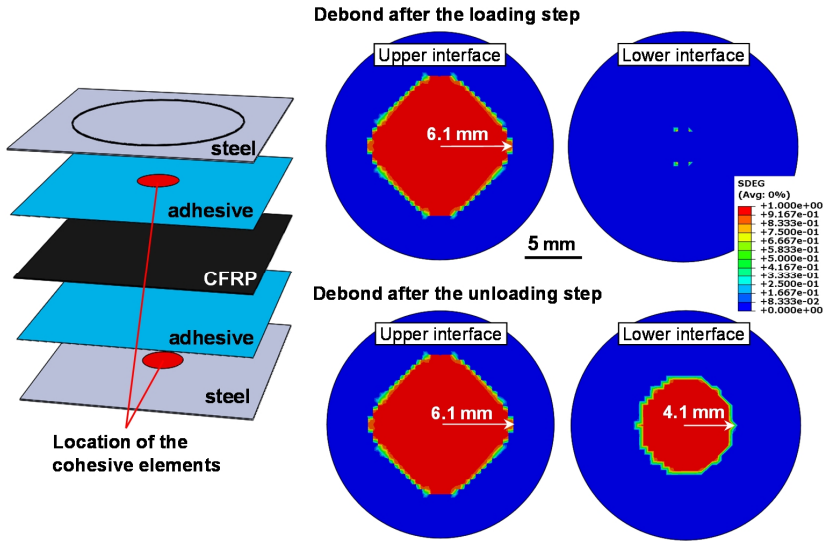


**Figure 4.8.** Debonding simulation in a CarbonFML specimen using cohesive zone modelling. The debond at the upper interface formed during the loading step, whereas the debond at the lower interface evolved mainly during the end part of the unloading step. SDEG represents the state of the damage evolution criterion (SDEG = 0 no damage, SDEG = 1 fully debonded).

In summary, the results of the debonding simulations suggest that debonding may initiate and propagate at the lower interface of the metal layer and the composite part during the early part of impact loading as a fracture mode II cracking. The shearing loads caused by the impactor contact are most likely the reason for the debonding to occur. The debond at the lower interface further propagates during the end part of the rebound phase as a result of peeling loads (fracture mode I -dominated cracking). The peeling loads are caused by the difference in the out-of-plane deformation tendencies of linear-elastic composite layers and elastic-plastic metal layers.

These findings set a new perspective on the results provided in the current literature. In many contexts, debonding in FMLs under impact loading is described as occurring purely due to the shearing loads. Such behaviour was explained among others by Wu and Yang (2005), who tested Glare FML specimens. However, the open crack shown in the cross-sectional images of their research at the interface of the lowermost metal sheet and the composite part implies possible participation of peeling loads within the debonding.

The findings of our research, on the other hand, support the discussion by Laliberté (2002) and Airoldi et al. (2009) that was introduced in Section 2.2. According to Laliberté, debonding initiation is a result of out-of-plane shear forces, but the debond may further propagate as the deformed metal sheets pull the structure apart. Airoldi et al. modelled debonding in Glare panels by CZM and found that debonding propagates during the loading and unloading steps. Therefore, our research offers further explanation for debonding occurring in FMLs during low-velocity impact loading.

Clearly, debonding characteristics are controlled by the stacking sequence and the materials of an FML. In addition, the debonding characteristics are dependent on the interfacial strength. If the interfacial strength is low, the mode II cracking during the loading step may propagate extensively at the metal-composite interface. The results of VCCT modelling in our background study (Pärnänen et al, 2015) showed mode I SERR values to drop drastically as the size of the pre-crack was increased. Therefore, a large debond that evolves during the loading step may limit further debonding at the lowermost interface during the unloading. Regardless, it is important to understand the source of the forces affecting at the interfaces, i.e. out-of-plane shear forces caused by the contact of an impactor and the peeling forces caused by the discrepancy in the loading response of the metal and composite layer in use.

### 4.2.4 The effects of debonding on impact response

The impact response in the context of this thesis refers to the impactor contact force–laminate's central deflection curve. The impact response has been an important result within impact engineering (Vlot, 1991; Laliberté, 2002; Morinière, 2014; Caprino et al., 2007). Therefore, the effects of debonding on the impact response of the CarbonFML specimens were studied in P4.

Exact control of debonding as well as composite damage in real FMLs is impossible. Therefore, the experimental responses of unbonded specimens and traditional FML specimens were first compared to understand the *emphasized* effect of debonding on the impact response. The unbonded specimens were prepared by using a release film in between the metal sheets and adhesive films. The traditional FML specimens had bonding between the layers and therefore they debonded naturally during the tests. The two types of specimens had different curing residual stresses inside the laminate. When the unbonded specimens had basically zero stress in the layers, the steel layers in the bonded specimens possessed tensile stress and the fibres compression stress. Morinière et al. (2013) have modelled the low-velocity impact of Glare specimens and concluded that residual stresses have a negligible effect on the impact response of FMLs when the maximum contact force and maximum displacement during the loading are studied.

Secondly, in p4, the *sole* effect of debonding on the impact response was dissected with two finite element models. The first model took into account only the plastic deformation of the metal layers. The second model was advanced to involve debonding at the upper and lower metal-composite interfaces by using cohesive elements.

The experimental results revealed that an initial debond reduces the curve slope of the contact force–central deflection curve significantly during the early part of the loading (Fig. 4.9). The result is expected, as the bending rigidity of the structure is reduced due to lack of any bonding. However, the response be-

came stiffer as the membrane stretching increased in the individual parts (layers). Based on the results of the simulations, the debonding during the loading step also reduces the curve slope as a result of increasing size of the damage (Fig. 4.9). In addition, the debonding during the unloading influences the end part of the contact force–central deflection curve as the lowermost metal sheet and the rest of the laminate are peeling apart. As the area under the contact force–central deflection curve at the maximum deflection equals the impact energy, the debonding will increase the ultimate deflection of the FML structure prior to the rebound phase.

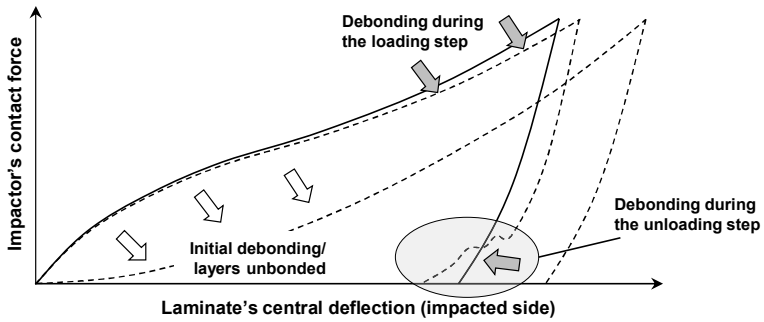


**Figure 4.9.** Schematics of the main findings about the effects of initial debonding (white arrows) and impact-induced debonding (grey arrows) on the impact response of CarbonFMLs.

Metal cracking and fibre failures have the strongest effect on the impact response (Laliberté, 2002). These damages are shown to typically form sharp drops in the contact force–central deflection curves (Vlot, 1991; Liu and Liaw, 2010; Caprino et al., 2004; Song et al., 2010). Delamination has been expected to occur during the early part of the loading, but the results in the impact response curve are somewhat unclear due to the oscillations caused by the impact (Caprino et al., 2004; Atas, 2007). On the other hand, Wu and Yang (2005) have concluded that delaminations and debonding might cause discrete drops in the load response curve after the first sharp drop due to extensive fibre failures. Hoo Fatt et al. (2003) and Morinière (2014) have also studied the impact response of unbonded FMLs. The results of these studies were similar to our findings as the initial curve slope was lower when compared to the bonded ones. Otherwise, the current literature outside this thesis offers very little information on the effects of debonding on the impact response.

### 4.2.5 The effect of debonding on the laminate's free surface straining

In addition to the impact response studies, strain measurements have been performed in the relevant literature to get insight into the impact damage process (Vlot, 1991; Laliberté, 2002; Seyed Yaghoubi et al., 2012; Zhu and Chai, 2012). In the literature, the strain measurements have been performed by using strain gauges at locations away from the impact point to study straining during the impact. Due to the nature of the strain gauges, the results cannot reveal the strain distribution over a large area. For this reason, we found it important to

study the post-impact strain field on the laminate's surface in P4 in order to understand the strain accumulation in FMLs during impact loading.

The digital image correlation (DIC) method was utilized to study the post-impact strain field on the back wall surface of the CarbonFML specimens. The measurements of a low impact energy CarbonFML (10 J) specimen revealed a highly strain-accumulated area close to the impact point ($r$ < 5 mm), see Fig. 4.10. The (radial and peripheral) strain distributions as a function of distance from the impact point were determined from the strain field results as well as by using two different FE simulations. The first model took into account only the plastic deformation of the metal layers. The second model was advanced to involve debonding at the upper and lower metal-composite interfaces by using cohesive elements. The results revealed that the debonding has the most drastic influence on the strains over the impact point – increasing the highest encountered post-impact strain. As the debond forms, the back wall metal sheet separates from the rest of the laminate, which allows high post-impact strains to remain on the metal surface. Thus, the debonding has a major influence on the post-impact stress state.

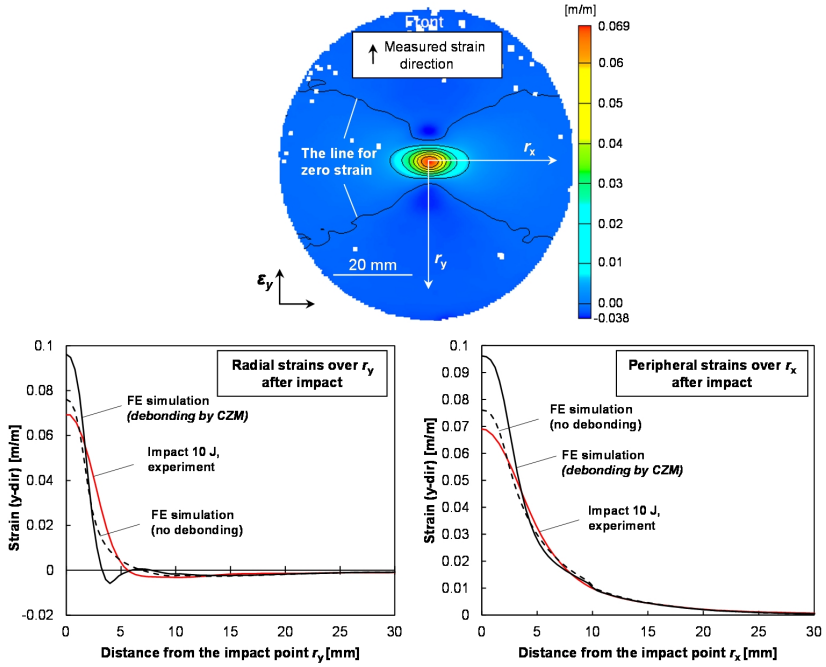


**Figure 4.10.** The measured post-impact strain field of a CarbonFML (10 J) specimen and the radial and peripheral strain distributions provided by the measurements and two FE simulations.

The effects of debonding on the surface straining were also studied at prescribed local points during indentation experiments and impact simulations (Fig. 4.11). The experimental strain gauge measurements on the bonded and unbonded specimens were performed to solve the *emphasized* effect of debonding. The simulations were solving the *sole* effect of debonding by using two different FE models. The first model took into account only the plastic deformation of the

metal layers. The second model was advanced to involve debonding at the upper and lower metal-composite interfaces by using cohesive elements. The measured peripheral strains at the distance of 20 mm from the impact point were remarkably lower throughout the contact period in the fully unbonded specimens when compared to the bonded specimens (Fig. 4.11). The simulated debonding during the impact loading was also shown to decrease peripheral strains, though the decrease was small compared to the emphasized effect observed in the experimental study.

The radial strains experienced a more radical change due to the initial debond. The unbonded specimens experienced positive strains right from the beginning. The bonding between the layers increased the bending rigidity of the panel and the bonded specimen experienced negative straining in the beginning of the impact event. Natural debonding, based on the simulation results, shifted the radial strain–displacement curve towards the response of the unbonded specimens. The simulated effect was similar for the peripheral strain; the radial strain change was small compared to the emphasized effect observed in the experimental results.

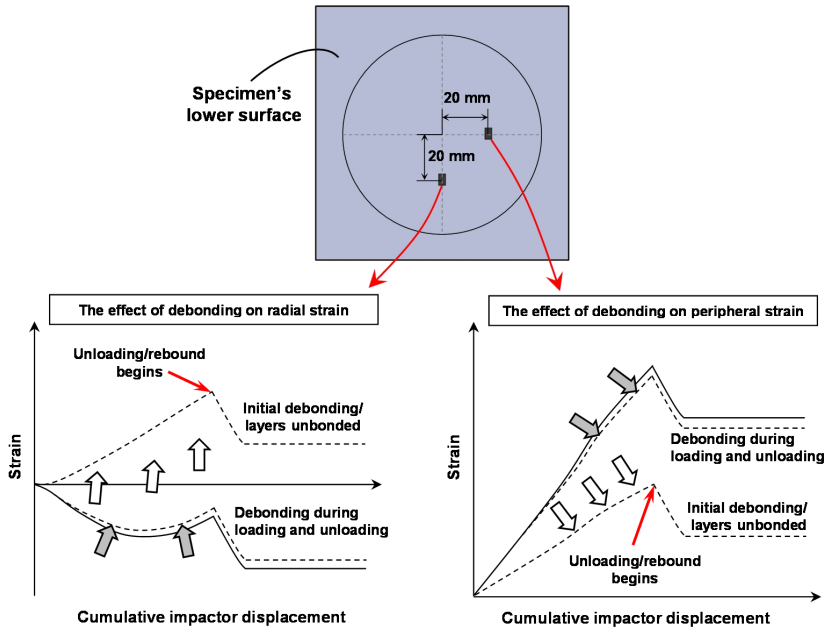


**Figure 4.11.** The schematic effect of debonding on the local straining at two locations (20 mm away from the impact point). The straining was studied via strain gauge measurements during indentation loading and also using FE simulations.

### 4.2.6 Strain rate effects

Loading due to impact subjects dynamic effects into the system, which can include (1) changes in the constituent material properties due to increased strain rates and (2) loads due to inertia, i.e. flexural and longitudinal waves (Davies and Olsson, 2004). Both metals and composites are rate sensitive materials

(Nicholas, 1981; Barré et al., 1996; Hsiao and Daniel, 1998; Gilat et al., 2002; Jacob et al., 2004; Armstrong and Walley, 2008). The level of sensitivity is dependent on the affecting strain rate, the studied material property as well as on the composition of the material. Therefore, it is important to discuss the relevance of strain rate effects on the results of Part II.

As an outcome of strain accumulation around the impact point, the strain rates will be uneven over the laminate's surface. A coarse estimate of the maximum radial strain rate for the CarbonFML 10 J specimen was 0.6 $s^{-1}$, based on the strain gauge data at 20 mm distance from the impact point. Based on the strain field results (see Fig. 4.10), a rough 'lower-limit' estimate for the average strain rate at the impact point is about 21 $s^{-1}$ (the peak post-impact strain being 0.069 m/m and the loading period of the impact being 3.3 ms). Clearly, the differences in strain rates are high over the whole test surface of an impact-loaded FML panel. The AISI 304L steel utilized in this research has been reported to increase its yield point by 40-60% when the strain rate increases to 25-50 $s^{-1}$ (Blandford et al., 2005). The mechanical properties of carbon fibres on the other hand are rather constant in a wide strain rate range (<1000 $s^{-1}$) (Davies and Olsson, 2004). Thus, the load response of steel will stiffen the CarbonFML during the impact loading, which was also observed from the test results (i.e. the curve slope was steeper for impact loaded specimen, see Fig. 4.12). Previously, Vlot (1991) and Zhou et al. (2016) found a similar increase in the curve slope when they compared the indentation and impact test results of aluminium based FMLs.

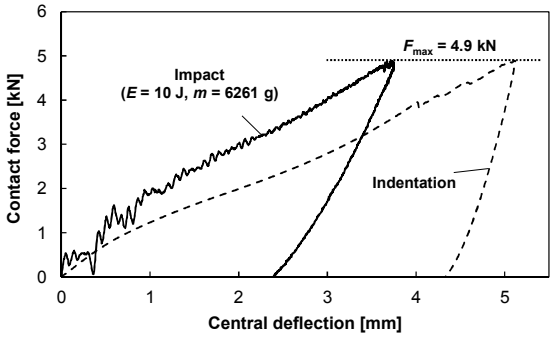


**Figure 4.12.** The contact force–central deflections responses of indentation (4.9 kN) and drop-weight impact loaded (10 J) CarbonFML specimens.

Results in the current literature also indicate load-rate dependent fracture toughness for the metal-polymer interfaces (Gent and Schultz, 1972; Kanerva, 2014), which suggests that the debonding characteristics of FMLs may be rate-dependent. Therefore, research needs to be continued in the dynamic environment to explain the (possible) effects of dynamics on the debonding.

Vlot et al. (1998) have suggested using strain rate strengthening fibres (increased ultimate stress/strain) in order to postpone fibre failure and, consequently, to improve the impact resistance of FMLs. As is shown in this thesis,

the in-plane post-impact strains and strain rates during impacts are highly peaked at the impact point. The peaked strains mean that the major in-plane damages (i.e. fibre failures and metal cracking) will initiate at the impact point. In order to further postpone the damage initiation, it would be beneficial to also have strain rate stiffening materials in FMLs (i.e. increased Young's modulus and yield limit while keeping high ultimate strain). The local stiffening would lead to increased material straining outside the impact point and hence lower the strain peak at the impact point. As a result, the damage initiation would become shifted towards higher impact energies, thus, the impact resistance would become higher.

# 5. Conclusions

## 5.1 Findings

The research of this thesis was divided into two parts. The first part (Part I) focused on studying the impact damage and simulation of an impact event. The impact damaging was studied experimentally using a wide range of impact energies to understand different phenomena. As a specific interest, the relation between the impact resistance and metal stress-strain response was studied. The results of P1 showed Glare 5 FML to possess a significantly higher specific energy limit for metal cracking when compared to MgFML panels. The difference in the specific energy limit was determined to result from the metal response over the plastic strain region. As the straining peaks at the impact point, a higher rate of strain hardening (i.e. the slope of the stress-strain curve at the plastic region) will enhance the in-plane load transfer of the FML away from the impact point. The enhanced load transfer lowers the ultimate strain at the impact point and increases the energy limit for metal cracking.

The second part (Part II) focused on the impact-induced debonding at the metal-composite interfaces. The main emphasis of the work was to understand the formation mechanisms of debonds. The full impact-damaging process of FMLs involves several different damage modes, and it is challenging to make explicit conclusions about the effects of individual damage modes. Therefore, a low-energy impact with a debonding-dominated damage was studied. Damage patterns were first resolved through an experimental post-impact damage assessment study. A finite element model taking into account debonding and metal plastic deformation was developed for simulations.

The experimental fracture surface analysis at the lower metal-composite interface suggested that the debonding crack tip near the impact point was fracture mode II loaded during propagation. In addition, there were indications of fracture mode I loading at the area outside the mode II loaded area. The simulations revealed that the debonding initiates as a fracture mode II cracking during the early part of the impact event. The out-of-plane shear forces induced by the impactor contact were concluded to be the source of the shearing crack tip loading. The debond further evolved as a fracture mode I -dominated cracking during the end part of the rebound phase. The peeling loads were determined to result from the discrepancy in the material response between the constituent layers (elastic-plastic metal and linear-elastic composite). In addition, the

debonding at the uppermost interface was studied using simulations. The results revealed that a debond tends to grow more extensively during the loading step when compared to the debonding at the lower interface during the loading step. The debond at the uppermost interface did not further evolve during the unloading step.

The effects of debonding on the impact response, i.e. on the impactor contact force–central deflection response, were also studied. The debonding during the loading phase of the impact event was shown to reduce the curve slope, i.e. to lower bending rigidity. The debonding during the rebound phase was noted to influence the end part of the unloading by amplifying the panel rebound, i.e. by decreasing the final deflection. For the first time, the post-impact strain fields over FMLs' surfaces were studied by experiments. The results revealed a highly strain accumulated area around the impact point ($r < 5$ mm). The highly accumulated strains were also found to lead to highly uneven strain rates over the laminate surface. In addition, the effects of debonding on the peripheral and radial strain components at the FML's lower surface were studied by using strain gauges. The debonding was shown to decrease the peripheral strain and to result in a positive change in the radial strain due to impact.

## 5.2 Work for the future

The research provoked questions regarding the impact resistance of FMLs. First, the role of the metal stress-strain curve for the impact resistance should be studied in detail to understand the quantitative effects of yield point and the rate of strain hardening. Also, the effect of strain rate sensitivity of constituent materials on the impact resistance is an interesting topic for future research.

Our models accounted for the debonding and metal plastic deformation. This simplification is a straightforward step as the debonding was the dominating damage mode based on the experiments. However, damage interaction should be studied in the future by introducing matrix cracking and composites delamination models into the FML modelling. Also, the debonding during the rebound phase is presumably dependent on whether or not major fibre damages and/or metal cracking occur during the loading phase. Therefore, also the interaction between the debonding and fibre fractures, as well as the interaction between the debonding and metal cracking should be further studied.

Based on this thesis, researchers of the field are suggested to take into account the debonding in the modelling of FMLs. The current study showed that the debonding during the rebound phase is a result of dissimilar material response of composite and metal layers (linear-elastic vs. elastic-plastic). Therefore, even when the debonding is taken into account in the modelling, the structure will have high internal stresses after an impact event. In the case that the debonding is not taken into account, the modelled internal stress and strain states in the

layers and global deformations of the panel will be highly unrealistic. An unrealistic prediction of post-impact stress/strain states and panel deformations will also lead to unrealistic predictions in post-impact strength analyses. Therefore, debonding should be part of the impact damage modelling when studying damage tolerance of FMLs after impact loading.

# Bibliography


Abrate, S. (2001). Modeling of impacts on composite structures. Composite Structures 51, 129–138.

Airoldi, A., Vesco, M., van der Zwaag, S., Baldi, A., Sala, G. (2009). Damage in glare laminates under indentation loads: experimental and numerical results. In: 17th International Conference on Composite Materials (ICCM17), Edinburgh, UK.

Alderliesten, R.C., Homan, J.J. (2006). Fatigue and damage tolerance issues of Glare in aircraft structures. International Journal of Fatigue 28 (10 SPEC. ISS.), 1116–1123.

Alderliesten, R., Rans, C., Benedictus, R. (2008). The applicability of magnesium based Fibre Metal Laminates in aerospace structures. Composites Science and Technology 68 (14), 2983–2993.

Armstrong, R.W., Walley, S.M. (2008). High strain rate properties of metals and alloys. International Materials Reviews, 53 (3), 105–128.

Asaee, Z., Taheri, F. (2016). Experimental and numerical investigation into the influence of stacking sequence on the low-velocity impact response of new 3D FMLs. Composite Structures 140, 136–146.

ASTM D5628. (2010). ASTM D5628-10, Standard Test Method for Impact Resistance of Flat, Rigid Plastic Specimens by Means of a Falling Dart (Tup or Falling Mass). ASTM International.

ASTM D7136. (2005). ASTM D 7136/D 7136M-05, Standard Teat Method for Measuring the Damage Resistance of a Fiber-Reinforced Polymer Matrix Composite to a Drop-Weight Impact Event. ASTM International.

ASTM D7137. (2005). ASTM D 7137/D 7137M-05, Standard Test Method for Compressive Residual Strength Properties of Damaged Polymer Matrix Composite Plates. ASTM International.

Atas, C. (2007). An Experimental Investigation on the Impact Response of Fiberglass/Aluminum Composites. Journal of Reinforced Plastics and Composites 26 (14), 1479–1491.

Barenblatt, G.I. (1962). The mathematical theory of equilibrium cracks in brittle fracture. Advances in Applied Mechanics, 7, 55–129.

Barré, S., Chotard, T., Benzeggagh, M.L. (1996). Comparative study of strain rate effects on mechanical properties of glass fibre-reinforced thermoset matrix composite. Composites Part A: Applied Science and Manufacturing, 27 (12), 1169–1181.

Bayandor, J., Thomson, R.S., Scott, M.L., Nguyen, M.Q., Elder, D.J. (2003). Investigation of impact and damage tolerance in advanced aerospace composite structures. International Journal of Crashworthiness 8 (3), 297–306.

Benzeggagh, M. L. and Kenane, M. (1996). Measurement of Mixed-mode Delamination Fracture Toughness of Unidirectional Glass/epoxy Composites with Mixed-mode Bending Apparatus. Composites Science and Technology, 56 (4), 439–449.

Bernhardt, S., Ramulu, M., Kobayashi, AS. (2007). Low-Velocity Impact Response Characterization of a Hybrid Titanium Composite Laminate. Journal of Engineering Material and Technology, 129, 220–226.

Blackman, B.R.K., Hadavinia, H., Kinloch, A.J., Williams, J.G. (2003). The use of cohesive zone model to study the fracture of fibre composites and adhesively-bonded joints. International Journal of Fracture, 119 (1), 25–46.

Blandford, R., Morton, D., Rahl, T., Snow, S. (2005). Impact Testing of Stainless Steel Materials. In: Proceedings of ASME Pressure Vessels and Piping, Division Conference, Denver, USA.

Burianek, D.A., Spearing, S.M. (2004). Delamination growth from face sheet seams in cross-ply titanium/graphite hybrid laminates. Composites Science and Technology 61 (2), 261–269.

Camacho, G.T., Ortiz, M. (1996). Computational modeling of impact damage in brittle materials. International Journal of Solids and Structures, 33 (20–22), 2899–2938.

Cantwell, W.J., Morton, J. (1991). The impact resistance of composite materials – a review. Composites 22 (5), 347–362.

Caprino, G., Spataro, G., Del Luongo, S. (2004). Low-velocity impact behaviour of fibreglass–aluminium laminates. Composites Part A – Applied Science and Manufacturing 35, 605–616.

Caprino, G., Lopresto, V., Iaccarino, P. (2007). A simple mechanistic model to predict the macroscopic response of fibreglass–aluminium laminates under low-velocity impact. Composites Part A – Applied Science and Manufacturing 38, 290–300.

Carrillo, J.G., Cantwell, W.J. (2008). Scaling effects in the low velocity impact response of fiber-metal laminates. Journal of Reinforced Plastics and Composites 28, 893–907.

Chai, G.B., Manikandan, P. (2014). Low velocity impact response of fibre-metal laminates – A review. Composite Structures 107, 363–381.

Cortes, P., Cantwell, W.J. (2005). The fracture properties of a fibre-metal laminate based on magnesium alloy. Composites: Part B, 37, 163–170.

Curiel Sosa, J.L., Karapurath, N. (2012). Delamination modelling of GLARE using the extended finite element method. Composites Science and Technology, 72 (7), 788–791.

Davies, G.A.O., Olsson, R. (2004). Impact on composite structures. The Aeronautical Journal, 108 (1089), 541–563.

Düring, D., Weiß, L., Stefaniak, D., Jordan, N., Hühne, C. (2015). Low-velocity impact response of composite laminates with steel and elastomer protective layer. Composite Structures 134, 18–26.

Dugdale, D.S. (1960). Yielding of steel sheets containing slits. Journal of Applied Mechanics, 8, 100–104.

Fan, J., Cantwell, W.J., Guan, Z.W. (2011a). The low-velocity impact response of fiber-metal laminates. Journal of Reinforced Plastics and Composites 30 (1), 26–35.

Fan, J., Guan, G.W., Cantwell, W.J. (2011b). Numerical modelling of perforation failure in fibre metal laminates subjected to low velocity impact loading. Composite Structures 93, 2430–2436.

Gent, A., Schultz, J. (1972). Effect of wetting liquids on the strength of adhesion of viscoelastic material. The Journal of Adhesion 3, 281–294.

Geubelle, P.H., Baylor J. (1998). Impact-induced delamination of composites: a 2D simulation. Composites Part B: Engineering, 29 (5), 589–602.

Gilat, A., Goldberg, R.K., Roberts, G.D. (2002). Experimental study of strain-rate-dependent behavior of carbon/epoxy composite. Composites Science and Technology, 62 (10–11), 1469–1476.

Guan, Z.W., Cantwell, W.J., Abdullah, R. (2009). Numerical Modeling of the Impact Response of Fiber–Metal Laminates. Polymer Composites 30 (5), 603–611.

Hagenbeek, M. (2001). Impact properties. In: Vlot, A., Gunnink, W. (eds.). Fibre Metal Laminates: An Introduction. Kluwer Academic Publishers. 407–426.

Hillerborg, A., Modeer M., Peterson P.E. (1976). Analysis of crack formation and growth in concrete by means of fracture mechanics and finite elements. Cement Concrete Research, 6, 773–782.

Hoo Fatt, M.S., Lin, C., Revilock Jr., D.M., Hopkins, D.A. (2003). Ballistic impact of GLARE™ fiber–metal laminates. Composite Structures 61, 73–88.

Hou, J.P., Petrinic, N., Ruiz, C., Hallett, S.R. (2000). Prediction of impact damage in composite plates. Composites Science and Technology 60, 273–281.

Hsiao, H.M., Daniel, I.M. (1998). Strain rate behavior of composite materials. Composites Part B: Engineering, 29 (5), 521–533.

Hühne, C., Petersen, E. (2014). Fiber-metal-laminates. In: Proceedings of the 13th European Conference on Spacecraft Structures, Materials & Environmental Testing (ESA SP-727), Braunschweig.

Jacob, G.C., Starbuck, J.M., Fellers, J.F., Simunovic, S., Boeman, R.G. (2004). Strain rate effects on the mechanical properties of polymer composite materials. Journal of Applied Polymer Science, 94 (1), 296–301.

Kanerva, M. (2014). Strength of rough interfaces: A micro-scale approach to steel-epoxy and composite systems. Dissertation, Aalto University, Finland.

Kolesnikov, B., Stefaniak, D., Wölper, J., Hühne, C. (2013). Payload adapter made from fiber-metal-laminate struts. In: Wiedemann M., Sinapius M. (eds.) Adaptive, Tolerant and Efficient Composite Structures, Springer-Verlag, Berlin Heidelberg, 263–274.

Krueger, R. (2004). Virtual crack closure technique: History, approach, and applications. Applied Mechanics Reviews, 57 (2), 109–143.

Laliberté, J.F. (2002). Investigation of Low-Velocity Impact Damage in Fibre-Metal-Laminates. Dissertation, Carleton University, Canada.

Laliberté, J.F., Straznicky, P.V., Poon, C. (2005). Impact Damage in Fiber Metal Laminates, Part 1: Experiment. AIAA Journal 43 (11), 2445–2453.

Lin, C., Hoo Fatt, M.S. (2006). Perforation of Composite Plates and Sandwich Panels under Quasi-static and Projectile Loading. Journal of Composite Materials 40 (20), 1801–1840.

Liu, Y., Liaw, B. (2010). Effect of Constituents and Lay-up Configuration on Drop-Weight Tests of Fiber-Metal Laminates. Applied Composite Materials, 17, 43–62.

Liu, Y., Seyed Yaghoubi, A., Liaw, B. (2014). Low-Velocity Impact Study on GLARE FMLs Using Various Indenters. Journal of Aerospace Engineering 27 (2), 325–335.

Marissen, R. (1988). Fatigue crack growth in ARALL: A hybrid aluminium-aramid composite material. Dissertation, Delft University of Technology, The Netherlands.

Mckown, S., Cantwell, W.J., Jones N. (2008). Investigation of scaling effects in fiber-metal laminates. Journal of Composite Materials 42, 865–88.

Moës, N., Dolbow, J., Belytschko, T. (1999). A finite element method for crack growth without remeshing. International Journal for Numerical Methods in Engineering, 46 (1), 131–150.

Morinière, F.D., Alderliesten, R.C., Sadighi, M., Benedictus, R. (2013). An integrated study on the low-velocity impact response of the GLARE fibre-metal laminate. Composite Structures 100, 89–103.

Morinière, F.D. (2014). Low-Velocity Impact on Fibre-Metal Laminates. Dissertation, Delft University of Technology, The Netherlands.

Morinière, R.D., Alderliesten, R.C., Benedictus, R. (2014). Modelling of impact damage and dynamics in fibre-metal laminates – A review. International Journal of Impact Engineering 67, 27–38.

Nakatani, H., Kosaka, T., Osaka, K., Sawada, Y. (2011). Damage characterization of titanium/GFRP hybrid laminates subjected to low-velocity impact. Composites Part A – Applied Science and Manufacturing 42, 772–781.

Needleman, A. (1987). A continuum model for void nucleation by inclusion debonding, Journal of Applied Mechanics, 54, 525–531.

Nicholas, T. (1981). Tensile testing of materials at high rates of strain. Experimental Mechanics, 21 (5), 177–185.

Olsson, R. (2000). Mass criterion for wave controlled impact response of composite plates. Composites Part A – Applied Science and Manufacturing 31, 879–887.

Payeganeh, G.H., Ashenai Ghasemi, F., Malekzadeh, K. (2010). Dynamic response of fiber-metal laminates (FMLs) subjects to low-velocity impact. Thin-Walled Structures, 48, 62–70.

Pärnänen, T., Jokinen, J., Kanerva, M., Saarela, O. (2015). Debonding modelling of indentation loaded fibre metal laminates. In: 10th International Conference on Composite Science and Technology (ICCST/10). Paper ID 155. Lisbon, Portugal.

Raju, I.S. (1987). Calculation of strain-energy release rates with higher order and singular finite elements. Engineering Fracture Mechanics 28 (3), 251–274.

Rice, J.R., Wang, J-S. (1989). Embrittlement of interfaces by solute segregation. Materials Science and Engineering: A, 107, 23–40.

Richardson, M.O.W., Wisheart, M.J. (1996). Review of low-velocity impact properties of composite material. Composites Part A – Applied Science and Manufacturing 27, 1123–1131.

Rybicki, E.F., Kanninen, M.F. (1977). A finite element calculation of stress intensity factors by a modified crack closure integral. Engineering Fracture Mechanics 9(4), 931–938.

Sadighi, M., Alderliesten, R.C., Benedictus R. (2012). Impact resistance of fiber-metal laminates: A review. International Journal of Impact Engineering, 49, 77–90.

Sarlin, E., Apostol, M., Lindroos, M., Kuokkala, V.-T., Vuorinen, J., Lepistö, T., Vippola, M. (2014). Impact properties of novel corrosion resistant hybrid structures. Composite Structures 108, 886–893.

Seo, H., Hundley, J., Hahn, H.T., Yang, J.-M. (2010). Numerical Simulation of Glass-Fiber-Reinforced Aluminum Laminates with Diverse Impact Damage. AIAA Journal 48 (3), 676–687.

Seyed Yaghoubi, A., Liu, Y., Liaw, B. (2012). Stacking Sequence and Geometrical Effects on Low-Velocity Impact Behaviors of GLARE 5 (3/2) Fiber–Metal Laminates. Journal of Thermoplastic Composite Materials, 25(2), 223–247.

Shi, Y., Swait, T., Soutis, C. (2012). Modelling damage evolution in composite laminates subjected to low velocity impact. Composite Structures 94, 2902–2913.

Song, S.H., Byun, Y.S., Ku, T.W., Song, W.J., Kim, J., Kang, B.S. (2010). Experimental and Numerical Investigation on Impact Performance of Carbon Reinforced Aluminum Laminates. Journal of Materials Science & Technology 26 (4), 327–332.

Tsamasphyros, G.J., Bikakis, G.S. (2011). Dynamic response of circular GLARE fiber-metal laminated subjected to low velocity impact. Journal of Reinforced Plastics & Composites 30 (11), 978–987.

Tsartsaris, N., Meo, M., Dolce, F., Polimeno, U., Guida, M., Marulo, F. (2011). Low-velocity impact behaviour of fiber metal laminates. Journal of Composite Materials 45 (7), 803–814.

Tvergaard, V., Hutchinson, J.W. (1992). The relation between crack growth resistance and fracture process parameters in elastic-plastic solids. Journal of the Mechanics and Physics of Solids, 40, 1377–1397.

van Rooijen, R.G.J. (2006). Bearing Strength Characteristics of Standard and Steel Reinforced GLARE. Dissertation, Delft University of Technology, The Netherlands.

Vlot, A. (1991). Low-velocity impact loading on fibre reinforced aluminium laminates (ARALL) and other aircraft sheet materials. Dissertation, Delft University of Technology, The Netherlands.

Vlot, A. (1996). Impact loading on fibre metal laminates. International Journal of Impact Engineering 18 (3), 291–307.

Vlot, A., Krull, M. (1997). Impact Damage Resistance of Various Fibre Metal Laminates. Journal de Physique IV Colloque 07 (C3), C3-1045–C3-1050.

Vlot, A., Kroon, E., La Rocca, G. (1998). Impact Response of Fiber Metal Laminates. Key Engineering Materials 141–143, 235–276.

Vlot, A., Vogelesang, V.B., de Vries, T.J. (1999). Towards application of fibre metal laminates in large aircraft. International Journal of Aircraft Engineering and Aerospace Technology 71(6), 558–570.

Vogelesang, L.B., Vlot, A. (2000). Development of fibre metal laminates for advanced aerospace structures. Journal of Materials Processing Technology, 103, 1-5.

Wu, G., Yang J.-M. (2005). The mechanical behavior of GLARE laminates for aircraft structures. The Journal of The Minerals, Metals & Materials Society, 57(1), 72-79.

Xu, X.P., Needleman, A. (1994). Numerical simulation of fast crack growth in brittle solids. Journal of the Mechanics and Physics of Solids, 42, 1397–1434.

Yarmohammad Tooski, M., Alderliesten, R.C., Ghajar, R., Khalili, S.M.R. (2013). Experimental investigation on distance effects in repeated low velocity impact on fiber-metal laminates. Composite Structures 99, 31–40.

Yu, G.-C., Wu, L.-Z., Ma, L., Xiong, J. (2015). Low velocity impact of carbon fiber aluminum laminates. Composite Structures 119, 757–766.

Zhu, S., Chai, G.B. (2012). Low-velocity impact response of fibre-metal laminates – Experimental and finite element analysis. Composites Science and Technology 72, 1793–1802.

Zhou, J., Guan, Z., Cantwell, W. (2014). Numerical modelling of perforation impact damage of fibre metal laminates. In: Proceedings of the 5th International Conference on Computational Methods (ICCM2014). Cambridge, England.

Zhou, J., Guan, Z.W., Cantwell, W.J. (2016). The influence of strain-rate on the perforation resistance of fiber metal laminates. Composite Structures, 125, 247–255.

Aalto-DD 262/2016

ISBN 978-952-60-7189-3 (printed)
ISBN 978-952-60-7188-6 (pdf)
ISSN-L 1799-4934
ISSN 1799-4934 (printed)
ISSN 1799-4942 (pdf)

**Aalto University**
**School of Engineering**
**Department of Mechanical Engineering**
**www.aalto.fi**

BUSINESS +
ECONOMY

ART +
DESIGN +
ARCHITECTURE

SCIENCE +
TECHNOLOGY

CROSSOVER

**DOCTORAL**
**DISSERTATIONS**